Syst. Biol. 68(6):859–875, 2019

DOI:10.1093/sysbio/syz023
Advance Access publication April 23, 2019

Sexual Dichromatism Drives Diversification within a Major Radiation of African Amphibians

DANIEL M. PORTIK[1,2*], RAYNA C. BELL[1,3], DAVID C. BLACKBURN[4], AARON M. BAUER[5], CHRISTOPHER D. BARRATT[6,7,8], WILLIAM R. BRANCH[9,10†], MARIUS BURGER[11,12], ALAN CHANNING[13], TIMOTHY J. COLSTON[14,15], WERNER CONRADIE[9,16], J. MAXIMILIAN DEHLING[17], ROBERT C. DREWES[18], RAFFAEL ERNST[19,20], ELI GREENBAUM[21], VÁCLAV GVOŽDÍK[22,23], JAMES HARVEY[24], ANNIKA HILLERS[25,26], MAREIKE HIRSCHFELD[25], GREGORY F. M. JONGSMA[4], JOS KIELGAST[27], MARCEL T. KOUETE[4], LUCINDA P. LAWSON[28,29], ADAM D. LEACHÉ[30], SIMON P. LOADER[31], STEFAN LÖTTERS[32], ARIE VAN DER MEIJDEN[33], MICHELE MENEGON[34], SUSANNE MÜLLER[32], ZOLTÁN T. NAGY[35], CALEB OFORI-BOATENG[36], ANNEMARIE OHLER[37], THEODORE J. PAPENFUSS[1], DANIELA RÖßLER[32], ULRICH SINSCH[17], MARK-OLIVER RÖDEL[25], MICHAEL VEITH[32], JENS VINDUM[18], ANGE-GHISLAIN ZASSI-BOULOU[38], AND JIMMY A. MCGUIRE[1]

[1]*Museum of Vertebrate Zoology, University of California, Berkeley, CA 94720, USA;* [2]*Department of Ecology and Evolutionary Biology, University of Arizona, Tucson, AZ 85721, USA;* [3]*Department of Vertebrate Zoology, National Museum of Natural History, Smithsonian Institution, Washington, DC 20560-0162, USA;* [4]*Florida Museum of Natural History, University of Florida, Gainesville, FL 32611, USA;* [5]*Department of Biology, Villanova University, 800 Lancaster Avenue, Villanova, PA 19085, USA;* [6]*Department of Environmental Sciences, University of Basel, Basel 4056, Switzerland;* [7]*German Centre for Integrative Biodiversity Research (iDiv) Halle-Jena-Leipzig, Leipzig 0413, Germany;* [8]*Max Planck Institute for Evolutionary Anthropology, Leipzig 0413, Germany;* [9]*Port Elizabeth Museum, P.O. Box 11347, Humewood 6013, South Africa;* [10]*Department of Zoology, Nelson Mandela Metropolitan University, P.O. Box 77000, Port Elizabeth 6031, South Africa;* [11]*African Amphibian Conservation Research Group, Unit for Environmental Sciences and Management, North-West University, Potchefstroom 2520, South Africa;* [12]*Flora Fauna & Man, Ecological Services Ltd. Tortola, British Virgin, Island;* [13]*Unit for Environmental Sciences and Management, North-West University, Potchefstroom 2520, South Africa;* [14]*Department of Biological Sciences, Florida State University, Tallahassee, FL 32306, USA;* [15]*Zoological Natural History Museum, Addis Ababa University, Arat Kilo, Addis Ababa, Ethiopia;* [16]*School of Natural Resource Management, Nelson Mandela University, George Campus, George 6530, South Africa;* [17]*Department of Biology, Institute of Sciences, University of Koblenz-Landau, Universitätsstr. 1, D-56070 Koblenz, Germany;* [18]*California Academy of Sciences, San Francisco, CA 94118, USA;* [19]*Museum of Zoology, Senckenberg Natural History Collections Dresden, Königsbrücker Landstr. 159, Dresden 01109, Germany;* [20]*Department of Ecology, Technische Universität Berlin, Rothenburgstr. 12, Berlin 12165, Germany;* [21]*Department of Biological Sciences, University of Texas at El Paso, El Paso, TX 79968, USA;* [22]*The Czech Academy of Sciences, Institute of Vertebrate Biology, Brno, Czech Republic;* [23]*Department of Zoology, National Museum, Prague, Czech Republic;* [24]*Pietermaritzburg, KwaZulu-Natal, South Africa;* [25]*Museum für Naturkunde, Leibniz Institute for Evolution and Biodiversity Science, Biodiversity Dynamics, Invalidenstr. 43, Berlin 10115, Germany;* [26]*Across the River – A Transboundary Peace Park for Sierra Leone and Liberia, The Royal Society for the Protection of Birds, 164 Dama Road, Kenema, Sierra Leone;* [27]*Natural History Museum of Denmark, University of Copenhagen, Universitetsparken 15, Copenhagen 2100, Denmark;* [28]*Department of Biological Sciences, University of Cincinnati, 614 Rieveschl Hall, Cincinnati, OH 45220, USA;* [29]*Life Sciences, Field Museum of Natural History, 1400 S. Lake Shore Dr., Chicago, IL 60605, USA;* [30]*Department of Biology, Burke Museum of Natural History and Culture, University of Washington, Seattle, WA, USA;* [31]*Life Sciences Department, Natural History Museum, London SW7 5BD, UK;* [32]*Biogeography Department, Trier University, Universitätsring 15, Trier 54296, Germany;* [33]*CIBIO Research Centre in Biodiversity and Genetic Resources, InBIO, Universidade do Porto, Campus Agrario de Vairão, Rua Padre Armando Quintas, No. 7, 4485-661 Vairão, Vila do Conde, Portugal;* [34]*Tropical Biodiversity Section, Science Museum of Trento, Corso del lavoro e della Scienza 3, Trento 38122, Italy;* [35]*Royal Belgian Institute of Natural Sciences, OD Taxonomy and Phylogeny, Rue Vautier 29, B-1000 Brussels, Belgium;* [36]*Forestry Research Institute of Ghana, P.O. Box 63, Fumesua, Kumasi, Ghana;* [37]*Département Origines et Evolution, Muséum National d'Histoire Naturelle, UMR 7205 ISYEB, 25 rue Cuvier, Paris 75005, France; and* [38]*Institut National de Recherche en Sciences Exactes et Naturelles, Brazzaville BP 2400, République du Congo*

[†]*Deceased.*

[*]*Correspondence to be sent to: Department of Ecology and Evolutionary Biology, University of Arizona, Tucson, AZ 85721, USA; E-mail: daniel.portik@gmail.com*

Received 27 July 2018; reviews returned 15 February 2019, 18 March 2019; accepted 9 April 2019
Associate Editor: Michael Alfaro

Abstract.—Theory predicts that sexually dimorphic traits under strong sexual selection, particularly those involved with intersexual signaling, can accelerate speciation and produce bursts of diversification. Sexual dichromatism (sexual dimorphism in color) is widely used as a proxy for sexual selection and is associated with rapid diversification in several animal groups, yet studies using phylogenetic comparative methods to explicitly test for an association between sexual dichromatism and diversification have produced conflicting results. Sexual dichromatism is rare in frogs, but it is both striking and prevalent in African reed frogs, a major component of the diverse frog radiation termed Afrobatrachia. In contrast to most other vertebrates, reed frogs display female-biased dichromatism in which females undergo color transformation, often resulting in more ornate coloration in females than in males. We produce a robust phylogeny of Afrobatrachia to investigate the evolutionary origins of sexual dichromatism in this radiation and examine whether the presence of dichromatism is associated with increased rates of net diversification. We find that sexual dichromatism evolved once within hyperoliids and was followed by numerous independent reversals to monochromatism. We detect significant diversification rate heterogeneity in Afrobatrachia and find that sexually dichromatic lineages have double the average net diversification rate of monochromatic lineages. By conducting trait simulations on our empirical phylogeny, we demonstrate that our inference of trait-dependent diversification is robust. Although sexual dichromatism in hyperoliid frogs is linked to their rapid diversification and supports macroevolutionary predictions of speciation by sexual selection, the function of dichromatism in reed frogs remains unclear. We propose that reed frogs are a compelling system for studying the roles of natural and sexual selection on the evolution of sexual dichromatism across micro- and macroevolutionary timescales. [Afrobatrachia; Anura; color evolution; diversification; macroevolution; sexual selection.]

In *The Descent of Man and Selection in Relation to Sex*, Darwin (1871) observed that many closely related taxa differed primarily in secondary sexual characters and suggested that sexual selection plays a role in the diversification of species. The concept of speciation through sexual selection was later developed into a theory that links the coevolution of secondary sexual traits and mating preferences to premating reproductive isolation (Lande 1981, 1982; Kirkpatrick 1982; West-Eberhard 1983). This conceptual framework predicts that both the strength of sexual selection and the prevalence of sexually selected traits have a positive association with speciation rate (Lande 1981, 1982; West-Eberhard 1983; Barraclough et al. 1995). If divergence in secondary sexual characters and sexual selection are indeed major drivers of speciation, then clades exhibiting elaborate sexually dimorphic traits and/or elevated sexual selection should display higher species richness and increased diversification rates at macroevolutionary scales. Empirically, these predictions have mixed support across a range of sexually dimorphic traits that serve as proxies for sexual selection (reviewed in Kraaijeveld et al. 2011), indicating that macroevolutionary trends for traits involved with intersexual signaling and mate-choice may differ from those more strongly influenced by intrasexual or natural selection. For example, traits under ecological selection such as body size dimorphism have no consistent relationship with diversification (Kraaijeveld et al. 2011), whereas sexual dichromatism, a form of sexual dimorphism in which the sexes differ in color, often functions as a mate recognition signal and is associated with diversification in several taxonomic groups (Misof 2002; Stuart-Fox and Owens 2003; Alfaro et al. 2009; Kazancıoglu et al. 2009; Wagner et al. 2012). Accordingly, sexual dichromatism has become a widely used proxy for studying the effects of sexual selection on speciation rate. However, phylogenetic comparative analyses explicitly testing for an association between sexual dichromatism and diversification have produced conflicting results, even in well-studied groups such as birds (Barraclough et al. 1995; Owens et al. 1999; Morrow et al. 2003; Phillimore et al. 2006; Seddon et al. 2013; Huang and Rabosky 2014) where sexual dichromatism plays an important role in signaling and mate-choice (Price 2008). Differences in methodologies and the spatial, temporal, and taxonomic scales among studies may partially explain these contrasting results. In particular, recent studies have highlighted concerns about the ability to distinguish between trait-dependent and trait-independent diversification scenarios using phylogenetic comparative methods (Rabosky and Goldberg 2015; Beaulieu and O'Meara 2016). In a broader sense, however, this disparity among studies may reflect more nuanced or novel mechanisms underlying the evolution of sexual dichromatism such that it does not consistently fit the conceptual framework of speciation by sexual selection. For instance, the striking sexual dichromatism in parrots of the genus *Eclectus* results from intrasexual competition to attract mates and intersexual differences in exposure to visual predators (Heinsohn et al. 2005). Likewise, the dynamic sexual dichromatism in frogs that form large breeding aggregations may serve to identify other competing males rather than to attract mates (Sztatecsny et al. 2012; Kindermann and Hero 2016; Bell et al. 2017b). Consequently, investigating the evolution of secondary sexual characters like dichromatism across ecologically diverse taxonomic groups is essential if we aim to generalize about the function of sexually dimorphic traits and better understand the roles of natural and sexual selection in biological diversification.

Secondary sexual traits are diverse and prevalent among anurans (frogs and toads) and include sexual size dimorphism, structures for acoustic signaling, nuptial pads, spines, elongated fingers, glands, and sexual dichromatism (Duellman and Trueb 1986). Sexual size dimorphism is common and occurs in >90% of species (Shine 1979; Han and Fu 2013), and body size evolution of the sexes is often attributed to fecundity for females and intrasexual competition, energetic constraints, agility, and predation for males (Salthe and Duellman 1973; Wells 1977; Shine 1979; Woolbright 1983; De Lisle and Rowe 2013; Han and Fu 2013; Nali et al. 2014). Male frogs of most species produce acoustic or vibrational signals to attract females, and these signals are essential for mate recognition and relaying social information (Ryan 1980; Gerhardt 1994; Gerhardt and Huber 2002). Structures like spines and tusks, which are present in males of many species, are used in male–male combat (e.g. McDiarmid 1975) whereas the diverse assortment of glands and nuptial pads, which are widespread in male frogs, are likely involved in courtship and amplexus (Duellman and Trueb 1986). In contrast to these widespread secondary sexual characters, anuran sexual dichromatism is rare, occurring in only ∼2% of frog species (Bell and Zamudio 2012; Bell et al. 2017b). Behavioral studies in a handful of frog species indicate that these sexual color differences may be subject to natural selection as well as inter- and intrasexual selection (Maan and Cummings 2009; Sztatecsny et al. 2012). Sexual selection on coloration has historically been dismissed in frogs with the assumption that communication is predominately acoustic (reviewed in Starnberger et al. 2014); however, several studies document the importance of color signals in courtship behavior and mate-choice, even in nocturnal species (Gomez et al. 2009, 2010; Jacobs et al. 2016; Yovanovich et al. 2017; Akopyan et al. 2018). If sexual dichromatism in frogs contributes to premating reproductive isolation, then sexually dichromatic clades may fit the conceptual framework of speciation by sexual selection and display higher species richness and increased diversification rates at macroevolutionary scales.

Afrobatrachia is a frog radiation (Arthroleptidae, Brevicipitidae, Hemisotidae, Hyperoliidae) that includes over 400 species distributed across sub-Saharan Africa that reflects much of the morphological,

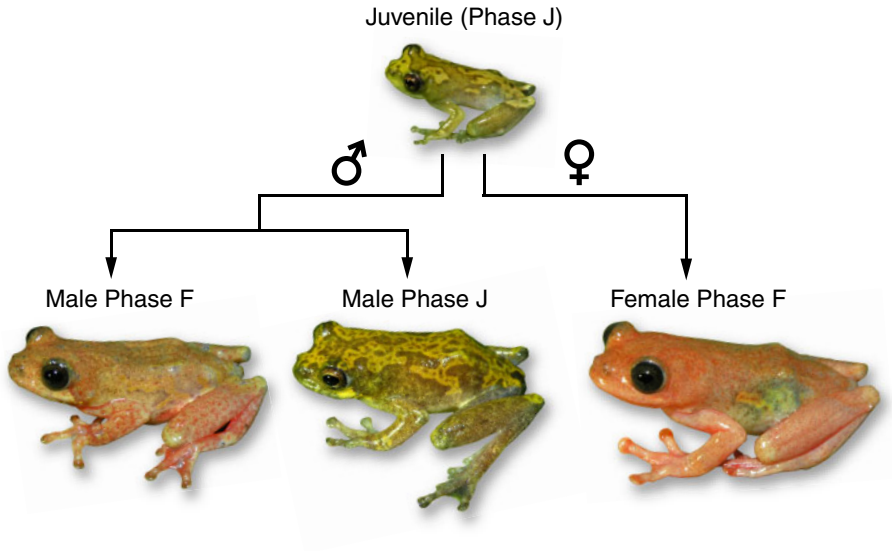

FIGURE 1. Illustration of ontogenetic color change occurring in hyperoliid frogs (*Hyperolius dintelmanni* shown) that underlies sexual dichromatism. In dichromatic species, females undergo a color change from Phase J to Phase F in response to steroid hormones at the onset of sexual maturity. Males retain the juvenile coloration (Phase J) or undergo a parallel change in color (to Phase F), however the proportion of the male color phases in populations varies across species. Secondary monochromatism can evolve from dichromatism through the loss of Phase J males (both sexes undergo an ontogenetic color change to Phase F) or through the loss of ontogenetic color change in both sexes (both sexes retain Phase J coloration at sexual maturity).

ecological, and reproductive mode diversity present in anurans (Portik and Blackburn 2016). Afrobatrachian frogs display many unusual secondary sexual characters including the hair-like skin structures of male Hairy Frogs (*Trichobatrachus*), an elongate third digit in males (up to 40% of body length in *Arthroleptis* and *Cardioglossa*), extreme body size dimorphism (*Leptopelis*, *Chrysobatrachus*, *Breviceps*), and prominent pectoral glands (*Leptopelis*) or gular glands on the male vocal sac (Hyperoliidae). Afrobatrachian frogs also have the highest incidence of sexual dichromatism among anurans, which is striking and prevalent in many hyperoliid reed frogs (*Hyperolius*, *Heterixalus*). In sexually dichromatic hyperoliids, the difference in coloration is female-biased: both sexes exhibit a consistent juvenile coloration upon metamorphosis (termed Phase J), but at the onset of maturity sex steroids trigger a color and/or color pattern change in females (Phase F), whereas males typically retain the juvenile color pattern (Fig. 1) (Schiøtz 1967; Richards 1982; Hayes 1997; Hayes and Menendez 1999). In many dichromatic reed frog species adult males can also display the Phase F coloration, but this generally occurs in lower frequency than the Phase J morph (Fig. 1) (Schiøtz 1967, 1999; Amiet 2012; Kouamé et al. 2015; Portik et al. 2016a). The function of the ontogenetic color shift in female reed frogs is poorly understood (Bell and Zamudio 2012), but it may be similar to female-biased sexual dichromatism in other vertebrates, which can result from a reversal in mating system in which females compete for males (Andersson 1994) or sexual niche partitioning in which males and females use different habitats (Shine 1989; Heinsohn et al. 2005). Alternatively, distinct female color patterns in reed frogs may play a role in courtship and mate recognition at breeding sites where upwards of 8 hyperoliid species congregate in a single night (Drewes and Vindum 1994; Kouamé et al. 2013; Portik et al. 2018). The link between sexual dichromatism and rapid speciation across disparate animal clades (Misof 2002; Stuart-Fox and Owens 2003; Alfaro et al. 2009; Kazancıoglu et al. 2009; Wagner et al. 2012) demonstrates that when sexual dichromatism functions primarily as an intersexual signal under strong sexual selection, there are predictable outcomes on diversification rate. Therefore, as a first step toward understanding the potential function of dichromatism in hyperoliids, including the plausibility of intersexual signaling, we aim to assess whether this trait fits the predictions of speciation by sexual selection on a macroevolutionary scale.

In this study, we reconstruct the evolutionary history of sexual dichromatism within Afrobatrachia and investigate whether diversification rate shifts in this continental radiation are associated with dichromatism. We produce a well-resolved species tree of Hyperoliidae from genomic data (>1000 loci) and greatly increased taxonomic sampling relative to previous studies (Wieczorek et al. 2000; Veith et al. 2009; Portik and Blackburn 2016). To explore the evolution of sexual dichromatism within the broader phylogenetic and biogeographic context of African frogs, we incorporate all published sequence data of Afrobatrachia to produce a robust, time-calibrated phylogeny. Using methods that improve the accuracy of character state reconstructions by accounting for trait and diversification rate heterogeneity (King and Lee

2015; Beaulieu and O'Meara 2016), we test the hypothesis that sexual dichromatism evolved repeatedly within Afrobatrachia (Veith et al. 2009). Finally, we estimate net diversification rates from our time-calibrated phylogeny using the hidden state speciation and extinction (HiSSE) framework (Beaulieu and O'Meara 2016). Specifically, we examine if diversification rate shifts occur within Afrobatrachia and if so, whether they are associated with the occurrence of sexual dichromatism. Given recent concerns raised about the ability to distinguish between trait-dependent and trait-independent diversification scenarios (Rabosky and Goldberg 2015; Beaulieu and O'Meara 2016), we assess the performance of available state-dependent diversification methods with a trait simulation study conducted using our empirical phylogeny.

Materials and Methods

Species Tree Estimation of Family Hyperoliidae

Taxonomic sampling.—We included 254 hyperoliid samples in our sequence capture experiment with multiple representatives per species when possible. Although there are 230 currently recognized hyperoliid species (AmphibiaWeb 2019), this family is in a state of taxonomic flux with recent studies recommending both the synonymy of species names and the splitting of species complexes (Rödel et al. 2002, 2003, 2009; Wollenberg et al. 2007; Schick et al. 2010; Conradie et al. 2012, 2013, 2018; Dehling 2012; Greenbaum et al. 2013; Liedtke et al. 2014; Loader et al. 2015; Portik et al. 2016a; Barratt et al. 2017; Bell et al. 2017a). We estimate that our sampling represents approximately 143 distinct hyperoliid lineages including 12 of 17 described hyperoliid genera. The 5 unsampled genera are either monotypic (*Arlequinus, Callixalus, Chrysobatrachus, Kassinula*) or species poor (*Alexteroon*, 3 spp.). Our sampling of the remaining genera is proportional to their recognized diversity and includes several known species complexes with lineages not reflected in the current taxonomy. We also sampled outgroup species from the following families: Arthroleptidae (7 spp), Brevicipitidae (1 sp), Hemisotidae (1 sp), and Microhylidae (1 sp). Museum and locality information for all specimens is provided in Supplementary Table S1 available on Dryad at http://dx.doi.org/10.5061/dryad.1740n0h.

Sequence capture data and alignments.—The full details of transcriptome sequencing, probe design, library preparation, sequence captures, and bioinformatics pipelines are described in Portik et al. (2016b), but here, we outline major steps of the transcriptome-based exon captures. We sequenced, assembled, and filtered the transcriptomes of 4 divergent hyperoliid species and selected 1260 orthologous transcripts for probe design. We chose transcripts 500–850 bp in length that ranged from 5% to 15% average pairwise divergence. Five additional nuclear loci (*POMC, RAG-1, TYR, FICD*, and *KIAA2013*) were also incorporated based on published sequence data (Portik and Blackburn 2016). The final marker set for probe design included 1265 genes from 4 species and 5060 individual sequences, with a total of 995,700 bp of target sequence. These sequences were used to design a MYbaits-3 custom bait library (MYcroarray, now Arbor Biosciences) consisting of 120 mer baits and a 2× tiling scheme (every 60 bp), which resulted in 60,179 unique baits. Transcriptomes, target sequences, and probe designs are available on Dryad (Portik et al. 2016c).

Genomic DNA was extracted using a high-salt extraction method (Aljanabi and Martinez 1997) and individual genomic libraries were prepared following Meyer and Kircher (2010) with modifications described in Portik et al. (2016b). Samples were pooled for capture reactions based on phylogenetic relatedness, and the combined postcapture libraries were sequenced on 3 lanes of an Illumina HiSeq2500 with 100 bp paired-end reads. Raw sequence data were cleaned following Singhal (2013) and Bi et al. (2012), and the cleaned reads of each sample were *de novo* assembled, filtered, and mapped as described in Portik et al. (2016b). The final filtered assemblies were aligned using MAFFT (Katoh et al. 2002, 2005; Katoh and Standley 2013) and trimmed using trimAl (Capella-Gutierrez et al. 2009). We enforced additional postprocessing filters for alignments, including a minimum length of 90 bp and a maximum of 30% total missing data across an alignment, resulting in 1047 exon alignments totaling 561,180 bp. Raw sequencing reads are deposited in the NCBI Sequence Read Archive (BioProject: PRJNA521610), newly generated sequences for the 5 captured nuclear loci are deposited in GenBank (Accession numbers: MK497946–MK499204), and all sequence capture alignments are available at https://osf.io/ykthm/.

Species tree estimation.—We used the sequence capture data set to estimate a species tree for Hyperoliidae using ASTRAL-III (Mirarab et al. 2014; Mirarab and Warnow 2015; Zhang et al. 2017), which uses unrooted gene trees to estimate the species tree. This method employs a quartet-based approach that is consistent under the multispecies coalescent process, and therefore appropriate for resolving gene tree discordance resulting from incomplete lineage sorting (Mirarab et al. 2014; Mirarab and Warnow 2015). This approach also allows for missing taxa in alignments, which were present in our sequence capture data and are problematic for other coalescent-based summary methods such as MP-EST (Liu et al. 2010). We kept samples with the most complete sequence data to collapse the alignments to a single representative per lineage and generated unrooted maximum likelihood (ML) gene trees with 200 bootstrap replicates for each locus using RAxML v8 (Stamatakis 2014) under the GTRCAT model. The set of 1047 gene trees was used to infer a species tree with ASTRAL-III, and node support was assessed with (i)

quartet support values, or local posterior probabilities computed from gene tree quartet frequencies, which also allows the calculation of branch lengths in coalescent units (Sayyari and Mirarab 2016), and (ii) 200 replicates of multilocus bootstrapping, where each of the 200 RAxML bootstrap trees per locus are used to infer a species tree and a greedy consensus tree is created from the 200 species trees to calculate percent support across nodes (Seo 2008).

Evolutionary Relationships of Afrobatrachian Frogs

DNA barcoding.—We obtained sequence data from the mitochondrial marker 16S ribosomal RNA (16*S*) for all samples included in the sequence capture experiment and for additional species that we were unable to include in our sequence capture experiment due to insufficient DNA yield. Polymerase chain reactions (PCRs) were carried out in 12.5 μL volumes consisting of: 1.25 μL Roche 10× (500 mM Tris/HCl, 100 mM KCl, 50 mM $(NH_4)_2$ SO_4, 20 mM $MgCl_2$, pH = 8.3), 0.75 μL 25 mM $MgCl_2$, 0.75 μL 2 mM dNTPs, 0.25 μL 10.0 μM forward primer, 0.25 μL 10.0 μM reverse primer, 8.40 μL H_2O, 0.10 μL Taq, and 0.75 μL DNA. Amplification involved initial denaturation at 94°C for 4 min, followed by 35 cycles of 95°C for 60 s, 51°C for 60 s, 72°C for 90 s, and a final extension at 72°C for 7 min, using the primer pairs 16SA and 16SB (Palumbi et al. 1991). The PCR amplifications were visualized on an agarose gel, cleaned using ExoSAP-IT, and sequenced using BigDye v3.1 on an ABI3730 sequencer (Applied Biosystems). Newly generated 16S sequence data are deposited in GenBank (Accession numbers: MK509481–MK509743).

GenBank data.—To expand our taxonomic sampling, we included all available published sequence data of afrobatrachian frogs. We built a molecular data matrix using the 5 nuclear loci included in our captures (*FICD, KIAA2013, POMC, TYR*, and *RAG-1*) and the mtDNA marker 16*S*. This resulted in the inclusion of 30 additional hyperoliids and 130 arthroleptid, brevicipitid, and hemisotid species, though many are represented solely by 16*S* mtDNA data. Nuclear loci were aligned using MUSCLE (Edgar 2004), and 16*S* sequences were aligned using MAFFT with the E-INS-i algorithm (Katoh et al. 2002, 2005). The final concatenated alignment of the expanded taxonomic data set consisted of 283 taxa and 3991 bp, with 36% total missing data.

Phylogenetic methods and divergence dating analyses.—We reconstructed the phylogenetic relationships of afrobatrachian frogs from the 5 nuclear genes and mtDNA data set using a ML approach in RAxML v8 (Stamatakis 2014). To preserve the relationships inferred with our species tree analyses of sequence capture loci, the sequence capture hyperoliid species tree containing 153 taxa (143 ingroup and 10 outgroup taxa) was used as a partial constraint tree for the ML analysis of the 283-taxon alignment of 6 loci. A preliminary step for our divergence dating analyses in BEAST v1.8.1 (Drummond et al. 2012) involved transforming the ML afrobatrachian frog tree to an ultrametric tree, and for this we used penalized likelihood with the "chronopl" function of APE (Sanderson 2002; Paradis et al. 2004), setting age bounds to allow divergence times to be compatible with our BEAST calibration priors. We performed BEAST analyses using a fixed ultrametric starting tree topology by removing relevant operators acting on the tree model. We used 4 secondary calibration points with normal distributions to constrain the most recent common ancestors (MRCAs) of Afrobatrachia to 80 Ma ± 5 SD, (Hemisotidae + Brevicipitidae) to 50 Ma ± 5 SD, Arthroleptidae to 40 Ma ± 5 SD, and Hyperoliidae to 40 Ma ± 5 SD. These secondary calibration points are based on a consensus of age estimates for afrobatrachian frogs resulting from multiple studies incorporating fossil calibrations and/or secondary calibrations (Roelants et al. 2007; Kurabayashi and Masayuki 2013; Loader et al. 2014; Portik and Blackburn 2016). We used the Yule model of speciation as the tree prior, applied an uncorrelated relaxed lognormal clock, and ran 2 analyses for 30,000,000 generations sampling every 3000 generations. Runs were assessed using TRACER v1.5.0 (Rambaut et al. 2013) to examine convergence, and a maximum clade credibility tree with median heights was created from 7500 trees after discarding a burn-in of 2500 trees.

Evolution of Sexual Dichromatism and State-Dependent Diversification

We scored the presence or absence of sexual dichromatism for hyperoliid species in our data set from multiple sources, including publications (Schiøtz 1967, 1999; Channing 2001; Channing and Howell 2006; Wollenberg et al. 2007; Rödel et al. 2009; Veith et al. 2009; Amiet 2012; Bell and Zamudio 2012; Channing et al. 2013; Conradie et al. 2013; Portik et al. 2016a), examination of museum specimens (Portik 2015), and the collective field observations from all authors. Sexual dichromatism in hyperoliids is quite pronounced and typically involves differences in both color and pattern. A species was considered sexually dichromatic if adult females and adult males exhibit distinct color patterns (Phase F and Phase J, respectively). We note that although many sexually dichromatic species also exhibit variation in male color phase (e.g., adult males in the population display Phase J and Phase F), the females of these dichromatic species consistently display one color phase (Phase F). A summary of the sexual dichromatism data is provided in Supplementary Table S2 available on Dryad.

We reconstructed the evolution of sexual dichromatism on the time-calibrated phylogeny of Afrobatrachia using Bayesian ancestral state reconstruction in BEAST (Drummond et al. 2012) and with HiSSE analyses using the R package HiSSE (Beaulieu and O'Meara 2016) (described below). We

performed Bayesian ancestral state reconstructions using several combinations of clock and character models in BEAST v1.8.1 (Drummond et al. 2012) following King and Lee (2015). The topology and branch lengths were fixed by removing all tree operators, and sexual dichromatism was treated as a binary alignment. Because all outgroup families are monochromatic, we fixed the root state by adding a placeholder monochromatic taxon to the root with a zero branch length, creating a hard prior distribution on the root where P(monochromatic root) =1, and P(dichromatic root) =0. A stochastic Mk model of character evolution (Lewis 2001) was used with symmetrical (Mk1) or asymmetrical (Mk2) transition rates between states, and each character model was analyzed using a strict clock (SC) model (enforcing a homogenous trait rate) and a random local clock model (allowing for heterotachy), resulting in 4 analysis combinations. The analyses involving the random local clock allowed estimation of the number and magnitude of rate changes using MCMC. All analyses were run for 200 million generations with sampling every 20,000 generations, resulting in 10,000 retained samples. We used the marginal likelihood estimator with stepping stone sampling, with a chain length of 1 million and 24 path steps, to estimate the log-marginal likelihood of each run (Baele et al. 2012, 2013). We performed 5 replicates per analysis to ensure consistency in the estimated log-marginal likelihood, and subsequently compared the 4 different analyses using log-Bayes factors, calculated as the difference in log-marginal likelihoods, to select the best fit clock model and character model combination. We summarized transitions between character states and created consensus trees to estimate the posterior probabilities of character states across nodes.

We performed HiSSE analyses using the R package HiSSE (Beaulieu and O'Meara 2016) to identify if sexual dichromatism in afrobatrachian frogs is associated with increased diversification rates, and to reconstruct ancestral states while accounting for transition rate and diversification rate heterogeneity. The HiSSE model builds upon the popular binary-state speciation and extinction (BiSSE) model (Maddison et al. 2007) by incorporating "hidden states" representing unmeasured traits that could impact the diversification rates estimated for states of the observed trait. The HiSSE model is therefore able to account for diversification rate heterogeneity that is not linked to the observed trait, while still identifying trait-dependent processes. The HiSSE framework also includes a set of null models that explicitly assume the diversification process is independent from the observed trait, without constraining diversification rates to be homogenous across the tree. The inclusion of these character-independent models circumvents a significant problem identified in the BiSSE framework, in which the simple "null" model of constant diversification rates is typically rejected in favor of trait-dependent diversification when diversification rate shifts unrelated to the trait occur in the phylogeny (Rabosky and Goldberg 2015; Beaulieu and O'Meara 2016). The improved character-independent diversification models, referred to as CID-2 and CID-4, contain the same number of diversification rate parameters as the BiSSE and HiSSE models, respectively. We fit 26 different models to our sexual dichromatism data set (Table 1): 6 represent BiSSE-like models, 4 are variations of the CID-2 model, 5 are variations of the CID-4 model, 9 are various HiSSE models with 2 hidden states, and 2 are HiSSE models with a single hidden state. One variation of CID-4 includes the 9-rate model developed by Harrington and Reeder (2017). Within each of these classes, the models vary mainly in the number of distinct transition rates (q), extinction fraction rates (ε), and net turnover rates (τ), and the most complex HiSSE model includes 4 net turnover rates, 4 extinction fraction rates, and 8 distinct transition rates. We enforced a monochromatic root state for all models and evaluated the fit of the 26 models using AIC scores, ΔAIC scores, and Akaike weights (ω_i) (Burnham and Anderson 2002). From the best-fit model, we estimated confidence intervals for relevant parameters and transformed ε and τ to obtain speciation (λ), extinction (μ), and net diversification rates using the "SupportRegion" function in HiSSE (Beaulieu and O'Meara 2016). We performed ancestral state estimations for each of the 26 models using the marginal reconstruction algorithm implemented in the "MarginRecon" function of HiSSE, again enforcing a monochromatic root state. Our final estimation and visualization of diversification rates and node character states on the afrobatrachian phylogeny took model uncertainty into account by using the model averaging approach described by Beaulieu and O'Meara (2016), such that model contributions to rates and states were proportional to their likelihoods.

Simulated traits and state-dependent diversification.—The identified bias toward the detection of trait-dependent diversification in the BiSSE framework (Rabosky and Goldberg 2015; Beaulieu and O'Meara 2016) prompted us to investigate if a similar outcome would be detected in our data set, and whether the HiSSE framework could improve our ability to distinguish whether the observed states are correlated with diversification rates. One concern raised by Beaulieu and O'Meara (2016) is that neutrally evolving traits simulated on trees generated from a complex heterogenous rate branching process can lead to false signals of trait-dependent diversification, signifying the HiSSE framework may be sensitive to particular types of tree shapes.

To evaluate the performance of these methods given our empirical tree topology, we simulated neutrally evolving traits on the afrobatrachian frog phylogeny and tested for trait-dependent diversification using both the BiSSE and HiSSE frameworks. We conducted independent simulations of a binary trait with the "sim.history" function in R package PHYTOOLS (Revell 2012) using the unequal rates *q*-matrices obtained from

TABLE 1. Summary of models and fits using HiSSE analyses, with sexual dichromatism as the observed state

Description	Model	Loglik	AIC	ΔAIC	wtAIC	Hidden States	State-dependent	Net turnover rates	Extinction fraction rates	Distinct transition rates
HiSSE	**19**	**−1033.5**	**2082.9**	**0.0**	**0.445**	**Yes**	**Yes**	**4**	**1**	**3**
HiSSE	15	−1026.0	2084.0	1.0	0.266	Yes	Yes	4	4	8
HiSSE	18	−1029.7	2085.4	2.5	0.130	Yes	Yes	4	1	8
CID-4	14	−1035.3	2086.5	3.6	0.075	Yes	No	4	1	3
CID-2	8	−1031.7	2087.3	4.4	0.049	Yes	No	2	2	8
HiSSE	16	−1033.5	2088.9	6.0	0.022	Yes	Yes	4	4	3
HiSSE	25	−1036.1	2092.2	9.3	0.004	only for state 0	Yes	3	3	4
CID-4	12	−1035.3	2092.5	9.6	0.004	Yes	No	4	4	3
CID-4	26	−1029.7	2093.4	10.4	0.002	Yes	No	4	4	9
CID-2	10	−1036.2	2094.4	11.5	<0.001	Yes	No	2	1	8
HiSSE	24	−1041.1	2102.3	19.3	<0.001	only for state 1	Yes	3	3	4
BiSSE-like	2	−1046.3	2102.6	19.7	<0.001	No	Yes	2	1	2
BiSSE-like	1	−1046.3	2104.6	21.7	<0.001	No	Yes	2	2	2
BiSSE-like	3	−1053.5	2115.1	32.1	<0.001	No	No	1	1	2
HiSSE	22	−1055.7	2121.5	38.5	<0.001	Yes	Yes	4	1	3
HiSSE	21	−1053.6	2127.2	44.3	<0.001	Yes	Yes	4	1	8
CID-4	13	−1060.2	2132.4	49.4	<0.001	Yes	No	4	1	1
HiSSE	20	−1061.9	2135.7	52.8	<0.001	Yes	Yes	4	1	1
HiSSE	17	−1060.4	2138.7	55.8	<0.001	Yes	Yes	4	4	1
CID-4	11	−1060.4	2138.8	55.8	<0.001	Yes	No	4	4	1
CID-2	9	−1068.1	2144.2	61.3	<0.001	Yes	No	2	1	1
CID-2	7	−1068.1	2146.2	63.3	<0.001	Yes	No	2	2	1
BiSSE-like	4	−1071.4	2152.8	69.8	<0.001	No	Yes	2	2	1
HiSSE	23	−1073.9	2153.7	70.8	<0.001	Yes	Yes	4	1	1
BiSSE-like	5	−1075.2	2158.3	75.4	<0.001	No	Yes	2	1	1
BiSSE-like	6	−1077.6	2161.2	78.3	<0.001	No	No	1	1	1

Note: The top ranked model is highlighted in bold.

our empirical data and enforcing a root state of trait absence. We required a minimum of 10% of taxa to exhibit the derived state and conducted simulations until we obtained 1500 replicates meeting this criterion. We used ML to fit a BiSSE model and the typical "null" model with equal speciation and extinction rates to each simulated trait using the R package DIVERSITREE (Maddison et al. 2007; FitzJohn et al. 2009; FitzJohn 2012). We performed likelihood ratio tests and calculated ΔAIC scores to determine if the constraint model could be rejected with confidence (ΔAIC > 2 or *P*-value < 0.05), and summarized the number of instances each of the 2 models was favored across the simulations. We analyzed the simulated data in the HiSSE framework as with our empirical data, but with a reduced set of 5 models representing each major category of model. This reduced model set included 2 BiSSE-like models that differed only in the constraint of τ, a CID-2 and CID-4 model, and a HiSSE model with 2 hidden states, 3 transition rates, equal ε, and distinct τ. We set a probability of one for trait absence at the root state to match the manner in which traits were simulated and evaluated the fit of the 5 models using ΔAIC scores and Akaike weights (ω_i) for each simulation, using a threshold of ΔAIC greater than 2 to favor a model. Specifically, we were interested in whether the unconstrained BiSSE-like or HiSSE models were favored, resulting in the detection of a false pattern of trait-dependent diversification, or if the CID-2 or CID-4 models were selected, capturing the expected pattern where the diversification process was independent from trait evolution.

RESULTS

Phylogenetic Relationships

The sequence capture data set consisting of 1047 loci and 561,180 bp produced a well-resolved species tree with a normalized quartet score of 0.877 and only 8 of 150 nodes (5%) with quartet scores below 0.9 (Supplementary Fig. S1 available on Dryad). The multilocus bootstrapping analysis produced similar results with low support for only 7 nodes, 6 of which also received low support in the species tree analyses (Supplementary Fig. S1 available on Dryad). The higher-level relationships recovered in the species tree are largely congruent with those recovered by Portik and Blackburn (2016), though we found strong support for a different placement of the genus *Acanthixalus* as sister to the clade containing *Semnodactylus*, *Paracassina*, *Phlyctimantis*, and *Kassina*, which together are sister to all other hyperoliids. Our improved sampling provides the first comprehensive assessment of evolutionary relationships within the speciose genera *Afrixalus* and *Hyperolius*. The monophyly of *Hyperolius* is supported, however *Afrixalus* is paraphyletic, and we found a sister relationship between the Ethiopian-endemic *Afrixalus enseticola* and the Malagasy-Seychelles species of *Heterixalus* and *Tachycnemis*, which are in turn sister to all remaining *Afrixalus* (Supplementary Fig. S1 available on Dryad). We found strong support for the southern African species *Hyperolius semidiscus* as sister to all other lineages in the genus, and furthermore recovered *Hyperolius parkeri*, *Hyperolius lupiroensis*, and

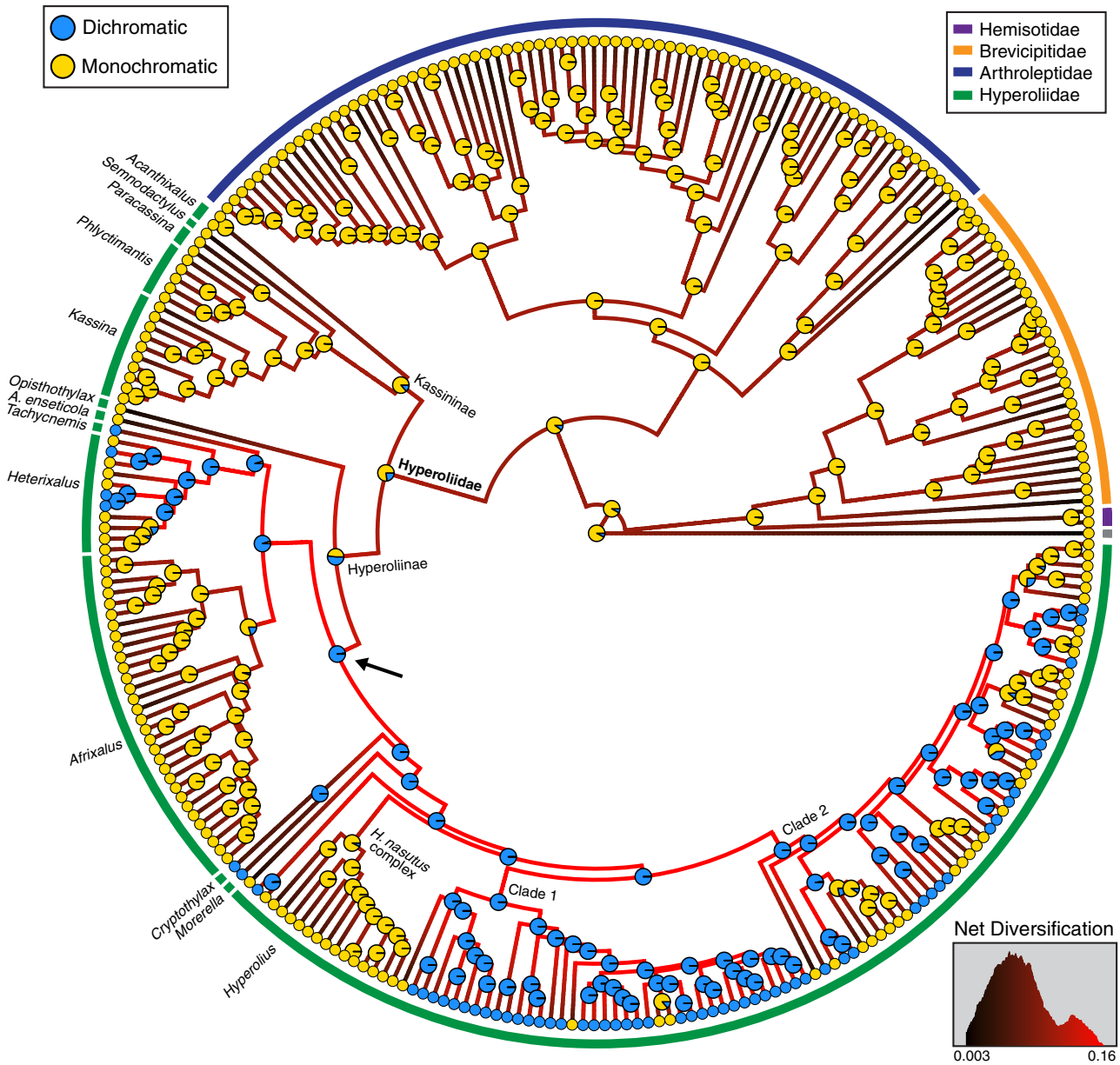

FIGURE 2. Ancestral state reconstruction of sexual dichromatism in afrobatrachian frogs from HiSSE using model averaging to account for uncertainty in both models and reconstructions. Circles at tips and nodes are colored by state with node pie charts indicating probability of a state assignment. Branches are colored using a gradient from the model-averaged net diversification rate, with black representing the slowest rate. The arrow highlights the node identified as displaying an unambiguous transition from monochromatism to sexual dichromatism.

the *Hyperolius nasutus* complex as sister to 2 larger subclades of *Hyperolius* (Clades 1 and 2; Fig. 2, Supplementary Fig. S1 available on Dryad). In an effort to distinguish the main division within Hyperoliidae, we recognize the subfamilies Kassininae Laurent, 1972 and Hyperoliinae Laurent, 1943 and define the content within each on the basis of our species tree analysis as follows: (i) Kassininae: *Acanthixalus*, *Kassina*, *Paracassina*, *Phlyctimantis*, and *Semnodactylus*; (ii) Hyperoliinae: *Afrixalus*, *Cryptothylax*, *Heterixalus*, *Hyperolius*, *Morerella*, and *Opisthothylax* (Fig. 2). We retain previous subfamily assignments for genera not sampled in our molecular study (Hyperoliinae: *Alexteroon*, *Arlequinus*, *Callixalus*, *Chrysobatrachus*, *Kassinula*), which should be included in future phylogenetic studies to confirm these placements.

The phylogenetic analyses of the Afrobatrachia supermatrix produced family-level relationships consistent with previous analyses (Pyron and Wiens 2011; Portik and Blackburn 2016; Feng et al. 2017), including a sister relationship between Hyperoliidae and Arthroleptidae, and between Hemisotidae and Brevicipitidae (Supplementary Fig. S2 available on

TABLE 2. Summary of trait rate analyses for the evolution of sexual dichromatism

Trait rate analysis	Log-marginal likelihood	Transitions 0 > 1	Transitions 1 > 0	Rate shifts	Rate minimum	Rate maximum
Strict clock Mk1	−92.12	15	7	–	–	–
Strict clock Mk2	−81.83	2	27	–	–	–
Relaxed local clock Mk1	−85.10	16	8	3.3	0.001	0.019
Relaxed local clock Mk2	−81.73	2	27	0.8	0.013	0.016

Note: For transition summaries, monochromatism is coded as "0" and dichromatism as "1." The average number of rate shifts is provided, rather than median.

Dryad). This expanded taxonomic data set also included improved sampling for the Malagasy hyperoliid genus *Heterixalus* and the *H. nasutus* complex, for which we recovered results consistent with Wollenberg et al. (2007) and Channing et al. (2013), respectively. We recovered an Eocene age for the time to most recent common ancestor (TMRCA) of the families Hyperoliidae, Arthroleptidae, and Brevicipitidae, of approximately 42.4 Ma (95% highest posterior density region [HPD]: 39.1–51.6 Ma), 45.4 Ma (95% HPD: 35.5–48.7 Ma), and 41.8 Ma (95% HPD: 33.9–49.8 Ma) (Supplementary Fig. S2 available on Dryad). These dates are younger than previous estimates (Roelants et al. 2007; Loader et al. 2014) but are consistent with more recent multilocus phylogenetic analyses (Portik and Blackburn 2016; Feng et al. 2017). We found diversification events began within Hyperoliinae approximately 35.8 Ma (95% HPD: 30.1–41.6 Ma) and within Kassininae approximately 38.3 Ma (95% HPD: 30.9–45.6 Ma). The majority of speciation events within *Hyperolius* occurred from the late Miocene to the Plio-Pleistocene (Supplementary Fig. S2 available on Dryad).

Evolution of Sexual Dichromatism and State-Dependent Diversification

We determined sexual dichromatism occurs in 60 of the 173 (34%) hyperoliid frog species included in our analyses. The greatest number of dichromatic species occurs in *Hyperolius* Clade 1 (35 of 39 species, 89%), followed by *Hyperolius* Clade 2 (18 of 50 species, 36%) and the genus *Heterixalus* (4 of 11 species, 36%) (Figs. 2 and 5). The Bayesian ancestral state reconstructions using 4 model combinations produced different patterns of character reconstructions and rates of trait evolution (Supplementary Fig. S3 available on Dryad). Overall, we found models with asymmetric character transition rates (Mk2) outperformed those with symmetric rates (Mk1), regardless of the clock model used (log-transformed Bayes factor range: 3.40–10.39; Table 2). The analysis with the highest log-marginal likelihood incorporated the relaxed local clock Mk2 model, though it was not a significantly better fit than the simpler SC Mk2 model (log-transformed Bayes factor of 0.10) indicating there is low variation in lineage-specific evolutionary rates for this trait. The ancestral character reconstructions of the SC Mk2 model indicated a median of 2 transitions from monochromatism to dichromatism. However, the character reconstructions revealed that this estimate is due to low posterior probability estimates for 2 critical nodes within Hyperoliinae (Supplementary Fig. S3 available on Dryad). The presence of dichromatism at one or both of these nodes results in a single origin of sexual dichromatism. In contrast, the SC Mk2 model demonstrated approximately 27 independent losses of sexual dichromatism within hyperoliids, including losses in entire groups (*Afrixalus*, *H. nasutus* complex) and numerous reversals within *Heterixalus* and *Hyperolius* (notably in Clade 2) (Supplementary Fig. S4 available on Dryad).

Our HiSSE analyses revealed that a HiSSE model with 4 net turnover rates, equal extinction fraction rates, and 3 distinct transition rates was the best-fit model (Model 19, Table 1). The second and third ranked models (ΔAIC of 1.0, 2.5) were also HiSSE models that varied in the number of extinction fraction rates or the number of transition rates. Together these 3 HiSSE models accounted for 84.1% of the model weight (Table 1) and support a signal of state-dependent diversification in which sexual dichromatism and a hidden state are associated with diversification rates. The net diversification rates inferred using the best-fit model were nearly twice as high in sexually dichromatic lineages (0.157) as compared with monochromatic lineages (0.091) in the absence of the hidden state (Fig. 3), and the combination of the hidden state and dichromatism or monochromatism resulted in much lower net diversification rate estimates (0.02 and <0.001, respectively). The trait reconstructions for all 4 state combinations indicated that the dichromatism plus hidden state combination occurs in the MRCA of 2 species-poor or monotypic genera (*Cryptothylax*, *Morerella*) (Supplementary Fig. S5 available on Dryad), and is associated with a markedly lower diversification rate (Fig. 3). The model-averaged ancestral state reconstructions demonstrated strong support for a single origin of sexual dichromatism and 25 independent reversals to monochromatism within Hyperoliinae, with reversal patterns similar to the Mk2 analyses (Fig. 2 and Supplementary Fig. S5 available on Dryad).

Simulated traits and state-dependent diversification.—Analyzed in the BiSSE framework, we found that many of the trait simulations on the phylogeny of Afrobatrachia resulted in the rejection of the "null" model of equal diversification rates across character

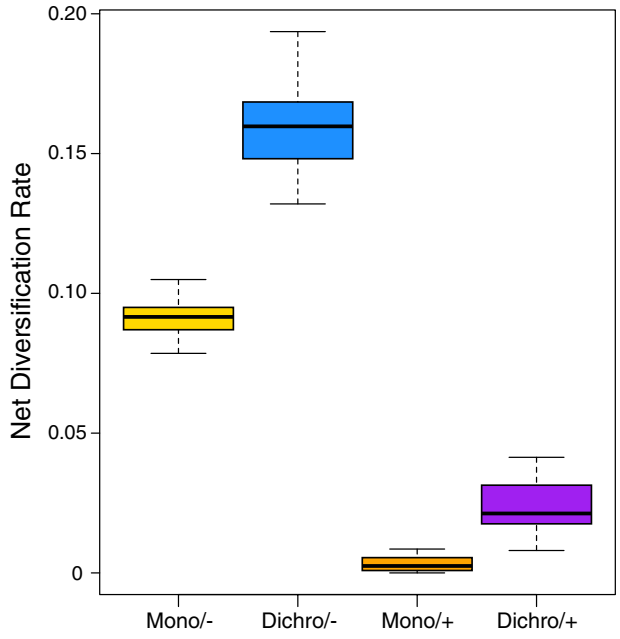

FIGURE 3. The net diversification rate confidence intervals estimated from the best-fit HiSSE model for various combinations of monochromatism, dichromatism, and the presence (+) or absence (−) of the hidden state.

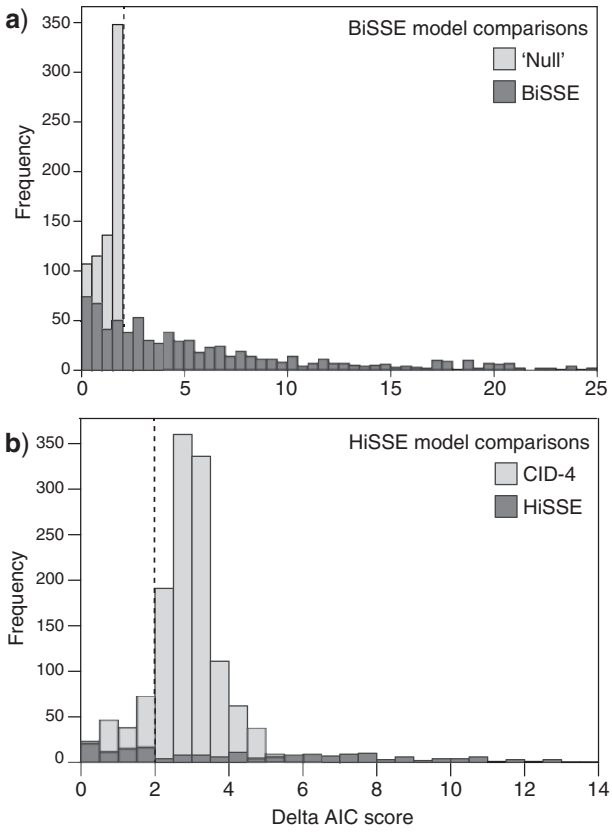

FIGURE 4. Histograms of the delta AIC comparisons resulting from (a) BiSSE analyses and (b) HiSSE analyses of the 1500 simulations of neutrally evolving traits on the Afrobatrachia phylogeny. The vertical dotted line represents a delta AIC of two. In the BiSSE analyses (a), delta AIC scores of less than two are considered a failure to reject the "null" model of constant diversification rates, whereas scores above two for the BiSSE model are interpreted as favoring a correlation between diversification rates and the simulated neutral trait. The HiSSE analyses (b) included 5 models, but only two were consistently selected as the top ranking, including the HiSSE and CID-4 (character-independent diversification) models. For these analyses delta AIC > 2 was considered as support for a particular model, whereas delta AIC < 2 was considered as equivocal support for the model.

states. Based on the significance of likelihood ratio tests, we rejected the "null" model in favor of trait-dependent diversification for 565 (37.6%) of our 1500 comparisons. We recovered similar results using a delta AIC cutoff value of 2, for which we found support for trait-dependent diversification in 546 (36.4%) of the simulations (Fig. 4). In many of these cases, we found unexpectedly strong support for the BiSSE model, and 160 (10.6%) of the comparisons resulted in delta AIC values ranging from 10 to 40.

In contrast to the BiSSE analyses, the addition of the character independent models (CID-2 and CID-4) in HiSSE dramatically reduced the detection of a false association between simulated traits and diversification rates by providing appropriate null models. In addition to the 2 CID models, our set of 5 models also included 2 BiSSE-like models and a typical HiSSE model. Based on a delta AIC cutoff value of 2, out of the 1500 analyses performed the CID-4 model was selected 1132 times (75.4%), the HiSSE model was chosen 125 times (8.3%), and the remaining 243 analyses (16.2%) showed equivocal support (ΔAIC = 0–2) for either the CID-4 or HiSSE model (Fig. 4). In the cases of equivocal support, the CID-4 and HiSSE models were always the top 2 models, which should be interpreted as a lack of support for trait-dependent diversification. Our error rate with the HiSSE model being favored in only 8.3% of our simulations was substantially lower than the Beaulieu and O'Meara (2016) "difficult tree" scenario in which the HiSSE model was favored in 29% of the data sets. These simulation results strongly suggest the branching pattern of our empirical phylogeny is not inherently problematic for the investigation of trait-dependent diversification using these available methods, adding support to our empirical analyses in which we detected an association between diversification rates and sexual dichromatism.

DISCUSSION

Hyperoliid Relationships and the Origin of Sexual Dichromatism

Afrobatrachian frogs account for more than half of all African amphibians and this continental radiation exhibits incredible variation in ecomorphology, reproductive mode, and other life history traits (Portik and Blackburn 2016). Within Afrobatrachia, the family Hyperoliidae is the most species-rich (~230 species) with surprisingly little diversity in ecomorphology and reproductive mode (Schiøtz 1967, 1999; Portik and Blackburn 2016), but with incredible variation in

coloration and sexual dichromatism. These phenotypic characteristics have generated considerable taxonomic confusion within hyperoliids (e.g., Ahl 1931), hindering a clear understanding of species diversity and the evolutionary history of this radiation. Here, we have produced the most comprehensive hyperoliid species tree to date and found support for an Eocene origin of 2 subfamilies representing a major division within Hyperoliidae: Kassininae (26 species) and Hyperoliinae (~200 species). Within Hyperoliinae, we clarified relationships within the hyperdiverse genus *Hyperolius* (~150 species), which consists of 2 major clades (Fig. 2, Supplementary Figs. S1 and S2 available on Dryad). These clades represent parallel radiations with species distributed across a variety of habitats and altitudes throughout sub-Saharan Africa, which showcases Hyperoliidae as a rich comparative framework for future biogeographic research.

Although both Kassininae and Hyperoliinae include colorful species, sexual dichromatism only occurs within Hyperoliinae where it is present in the genera *Tachycnemis, Cryptothylax*, and *Morerella*, several species of *Heterixalus*, and more than half of the *Hyperolius* species we sampled (Fig. 2, Supplementary Table S2 available on Dryad). A previous study hypothesized that sexual dichromatism evolved multiple times within Hyperoliidae (Veith et al. 2009); however, we found overwhelming support for a single origin of sexual dichromatism (Fig. 2, Supplementary Fig. S3 available on Dryad) and over 20 independent reversals to monochromatism that range from early transitions that characterize entire genera (e.g., *Afrixalus*) to recent reversals within *Heterixalus* and *Hyperolius* (Fig. 2, Supplementary Fig. S4 available on Dryad). This transition bias from dichromatism to monochromatism also occurs in birds (Price and Birch 1996; Omland 1997; Burns 1998; Kimball et al. 2001; Hofmann et al. 2008; Dunn et al. 2015; Shultz and Burns 2017), in which secondary monochromatism can evolve as the result of a color change in either sex (Kimball and Ligon 1999; Johnson et al. 2013; Price and Eaton 2014; Dunn et al. 2015). Similar transitional pathways to secondary monochromatism occur in hyperoliids, in which females may lose the ability for color transformation at sexual maturity (both sexes retain the Phase J juvenile coloration) or males undergo obligatory ontogenetic color change at maturity (both sexes develop Phase F coloration) (Figs. 1, 5). Characterizing juvenile coloration across species (which remains unknown in many hyperoliids) and documenting ontogenetic color change (including the prevalence of male color phases, e.g., Portik et al. 2016a) will be essential steps toward differentiating between these 2 forms of monochromatism. In experimental settings, the hormone estradiol induces color transformation in both sexes in the dichromatic species *Hyperolius argus* and *Hyperolius viridiflavus*. Conversely, the effects of testosterone appear to differ across species (Richards 1982; Hayes and Menendez 1999), suggesting that evolutionary transitions from dichromatism to monochromatism result directly from differences in hormone sensitivities among species. Reversals to monochromatism are especially prominent in *Hyperolius* Clade 2 (12 independent events; Fig. 2, Supplementary Fig. S4 available on Dryad), highlighting the potential for future research in this group to identify the physiological basis and molecular underpinnings of these transitions. For example, 3 monochromatic species of the *Hyperolius cinnamomeoventris* complex that are endemic to the islands of São Tomé and Príncipe (*Hyperolius drewesi, Hyperolius molleri, Hyperolius thomensis*; both sexes with Phase F coloration) are derived from a mainland clade containing a mix of sexually dichromatic species (*Hyperolius cinnamomeoventris, Hyperolius olivaceus*; females Phase F, males Phase J) and monochromatic species (*Hyperolius veithi*; both sexes Phase J) (Fig. 5). Variation among these closely related species is well suited for investigating both the evolutionary and ecological contexts underlying transitions from sexual dichromatism to monochromatism.

Sexual Dichromatism Is Linked to Increased Diversification Rates

Sexual dichromatism is an important predictor of diversification in several taxonomic groups including cichlids (Wagner et al. 2012), labrid fishes (Alfaro et al. 2009; Kazancıoglu et al. 2009), agamid lizards (Stuart-Fox and Owens 2003), and dragonflies (Misof 2002). There is no such association in bees (Blaimer et al. 2018), and in birds the relationship between dichromatism and species richness/speciation rate varies among studies that differ in methodology and taxonomic scale (Barraclough et al. 1995; Owens et al. 1999; Morrow et al. 2003; Phillimore et al. 2006; Seddon et al. 2013; Huang and Rabosky 2014). Some state-dependent speciation and extinction model sets, such as the BiSSE method, are no longer considered adequate for robustly detecting trait-dependent diversification (Rabosky and Goldberg 2015; Beaulieu and O'Meara 2016). In contrast to BiSSE, the HiSSE method contains an expanded model set that can link diversification rate heterogeneity to observed traits, hidden traits, or character independent processes. In particular, the inclusion of appropriate null models (character-independent models) reduces the inference of trait-dependent diversification when a phylogeny contains diversification rate shifts unrelated to the focal trait (Beaulieu and O'Meara 2016). Our trait simulation study recapitulated this result (Fig. 4) while demonstrating that the branching pattern of our Afrobatrachia phylogeny is unlikely to drive false inferences of trait-dependent diversification using HiSSE (e.g., the "worst-case" scenario of Beaulieu and O'Meara 2016). We found that sexually dichromatic hyperoliid lineages have nearly double the average diversification rate of monochromatic lineages, and that these diversification rates are not inflated by a hidden trait. The shift to the sexual dichromatism plus hidden state character combination occurred only once in the common ancestor of 2 genera (*Cryptothylax,*

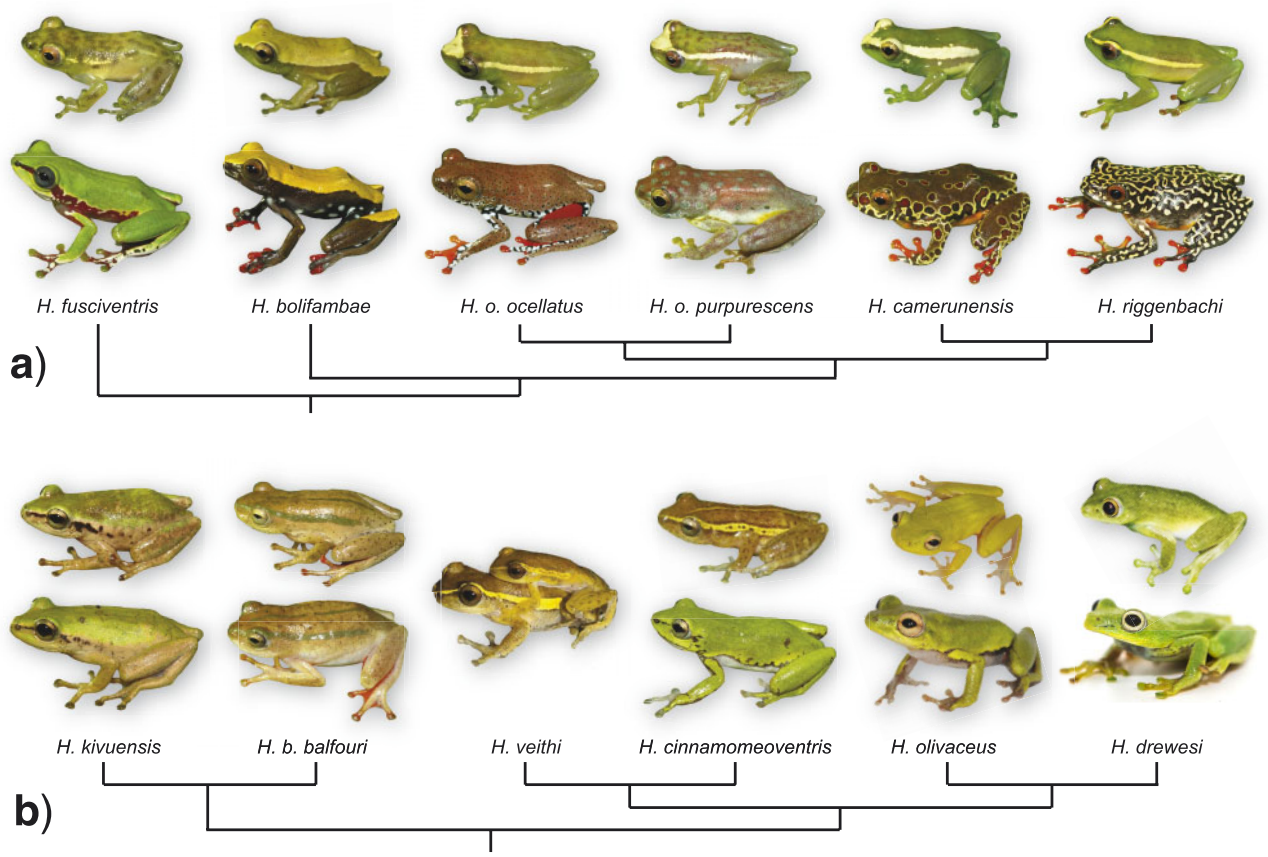

FIGURE 5. Illustration of (a) several *Hyperolius* species in the predominately sexually dichromatic Clade 1 and (b) several *Hyperolius* species in Clade 2 that exhibit multiple transitions to secondary monochromatism. Males are positioned in the top rows, with females below, and the phylogenetic relationships among species are depicted (though not all taxa have been included) Photo credits: Daniel Portik, Jos Kielgast, Bryan Stuart, Andrew Stanbridge.

Morerella; Supplementary Fig. S5 available on Dryad) and is actually associated with lower diversification rates (Fig. 3). Together, our results demonstrate that diversification rate heterogeneity occurs within Afrobatrachia, and that the origin and persistence of sexual dichromatism in hyperoliid frogs is linked to their rapid diversification across sub-Saharan Africa.

How Does Sexual Dichromatism Influence Diversification Rate?

Sexual dichromatism is a common proxy for sexual selection in macroevolutionary studies (reviewed in Kraaijeveld et al. 2011), especially for testing the prediction that clades with variation in secondary sexual characters under strong sexual selection exhibit higher diversification rates and species richness (Lande 1981, 1982; West-Eberhard 1983; Barraclough et al. 1995). Although our trait-dependent diversification analyses strongly support a faster rate of net diversification associated with sexual dichromatism, we currently lack behavioral and natural history data in hyperoliids to establish whether sexual dichromatism is actually under strong sexual selection. At more recent timescales, speciation by sexual selection can result in a group of closely related species with high ecological similarity but differing almost exclusively in signaling traits (West-Eberhard 1983; Dominey 1984; Panhuis et al. 2001; Turelli et al. 2001; Andersson 1994; Mendelson and Shaw 2012; Ritchie 2007; Safran et al. 2013). Among frog species with similar morphologies (e.g., treefrogs), ecological divergence primarily results from changes in body size. Frogs are generally opportunistic, gape-limited predators (Duellman and Trueb 1986), and in hyperoliids food partitioning is strongly dictated by body size (Luiselli et al. 2004). At one well-characterized community site, the females of 7 sexually dichromatic *Hyperolius* species display minimal differences in body size (Portik et al. 2018) but exceptional divergence in color (Portik et al. 2016a). Five of these species occur in *Hyperolius* Clade 1, and within this clade there tend to be striking interspecific color differences in females, but not males, among closely species (Fig. 5). This pattern of interspecific variation in secondary sexual characters in the absence of ecological divergence is consistent with the predictions of speciation by sexual selection. By inference, this would imply that dichromatism in hyperoliids—specifically female color—is an essential mate recognition signal (*sensu* Mendelson and Shaw 2012). In frogs, male calls are well-established mate

recognition signals that can be under strong sexual selection (Ryan 1980; Gerhardt 1994), and these acoustic signals are demonstrably important for hyperoliid frogs. Males form dense breeding aggregations and choruses (Bishop et al. 1995), calls differ between closely related species (Schiøtz 1967, 1999; Gilbert and Bell 2018) and females prefer conspecific calls over calls of syntopic heterospecifics (Telford and Passmore 1981). However, visual displays can also serve as important courtship signals in frogs, typically in conjunction with acoustic signaling (Gomez et al. 2009, 2010; Starnberger et al. 2014; Jacobs et al. 2016; Yovanovich et al. 2017; Akopyan et al. 2018). Although most studies have documented female preference for male coloration, the recent discovery of female displays during nocturnal phyllomedusine treefrog courtship highlights the possibility of male mate-choice and intersexual selection of female coloration (Akopyan et al. 2018). The notable lack of heterospecific matings among dichromatic species at high-diversity breeding sites (Portik et al. 2018) strongly suggests behavioral isolation may be linked to divergent mate recognition signals, including male call (Telford and Passmore 1981), gular gland compounds (Starnberger et al. 2013), or female coloration. Our knowledge of reproductive behavior in hyperoliids is largely based on a single dichromatic species (*H. marmoratus*; Dyson and Passmore 1988; Telford and Dyson 1988; Dyson et al. 1992; Jennions et al. 1995), and as such there may be an overlooked role for mutual mate-choice in hyperoliids in which females locate males by call and/or pheromones and males assess color patterns of approaching females.

Although it can be tempting to equate sexually dimorphic traits such as dichromatism with sexual selection, several alternative mechanisms may also contribute to female-biased dichromatism in hyperoliids. For instance, aposematism is a widespread anti-predator mechanism in frogs that is typically accompanied by the presence of skin toxins (reviewed in Toledo and Haddad 2009; Rojas 2017) such as alkaloids (Daly 1995). Sex-specific differences in chemical defense have been documented in some frogs (Saporito et al. 2010; Jeckel et al. 2015), but in several dichromatic hyperoliid species neither sex contained alkaloids in their skin (Portik et al. 2015). This finding suggests that either aposematism is an unlikely explanation for ornate coloration or that hyperoliids have evolved novel compounds for chemical defense. Female-biased dichromatism has also been tied to sex-role reversal in fishes and birds (Roede 1972; Oring 1982; Berglund et al. 1986a,b; Eens and Pinxten 2000), in which females compete more intensely than males for access to mates. This mechanism seems unlikely for hyperoliids because males in both monochromatic and dichromatic species form dense choruses and compete intensely to attract females, often engaging in combat (Telford 1985; Backwell and Passmore 1990). Finally, sexual niche partitioning (Selander 1966; Shine 1989) can result in sexual dichromatism when the sexes use different microhabitats, and as a consequence are subject to different selective pressures and predation regimes (Heinsohn et al. 2005; Bell and Zamudio 2012). During the breeding season, male hyperoliids are exposed on calling sites and Hayes (1997) proposed that more cryptic male coloration may reduce predation pressure. This hypothesis is consistent with a greater number of observations of predation events on females of dichromatic species (Grafe 1997; Portik et al. 2018). Quantifying differences in predation rates between the sexes, between monochromatic and dichromatic species, and between Phase F and Phase J males within dichromatic species would address whether this aspect of natural selection is also shaping the evolution of sexual dichromatism. Although these mechanisms and other differences in natural selection pressures may influence the evolution of sexual dichromatism in hyperoliids, they are generally not expected to elevate rates of reproductive isolation or drive diversification rate shifts comparable to the effects of sexual selection. Therefore, we propose that hyperoliids are a compelling system for disentangling the roles of sexual selection and natural selection in the evolution of sexual dichromatism, and how these mechanisms have promoted diversification at both microevolutionary and macroevolutionary timescales.

Supplementary Material

Data available from the Dryad Digital Repository: http://dx.doi.org/10.5061/dryad.1740n0h.

Funding

Molecular data collection by DMP was funded by a National Science Foundation Doctoral Dissertation Improvement Grant (DEB: 1311006), an Ecological, Evolutionary, and Conservation Genomics Research Award presented to DMP by the American Genetic Association, a National Science Foundation grant (DEB: 1202609) awarded to DCB, a UC Berkeley President's Postdoctoral Fellowship awarded to RCB, and by the Museum of Vertebrate Zoology.

Acknowledgments

We thank the following institutions for accessioning field collections and for facilitating loan access: California Academy of Sciences, Cornell University Museum of Vertebrates, Institut National de Recherche en Sciences Exactes et Naturelles, Museum für Naturkunde, Berlin, Museùm National d'Histoire Naturelle, Museum of Comparative Zoology, Museum of Vertebrate Zoology, National Museum Prague, Natural History Museum London, North Carolina Museum of Natural Sciences, Port Elizabeth Museum, Senckenberg Natural History Collections Dresden, South African Institute for Aquatic Biodiversity, South African

National Biodiversity Institute, The Field Museum, Trento Museum of Science, University of Texas at El Paso Biodiversity Collections, and the Zoological Natural History Museum, Addis Ababa University. All authors express thanks to the many government agencies, ministries, and departments that issued research permits and provided the access necessary to conduct their individual field work in sub-Saharan Africa. This work used the Vincent J. Coates Genomics Sequencing Laboratory at UC Berkeley, supported by NIH S10 Instrumentation Grants S10RR029668 and S10RR027303.

Data Accessibility

Raw sequencing reads are deposited in the NCBI Sequence Read Archive (BioProject: PRJNA521610), newly generated sequences for the 5 captured nuclear loci and 16S are deposited in GenBank (Accession numbers: MK497946–MK499204; MK509481–MK509743), and the sequence capture alignments are available at https://osf.io/ykthm/. We developed a project page (https://osf.io/yeu38) using the Open Science Framework that includes all data, scripts, and instructions required to replicate our analyses. We include all relevant material for the species tree analyses (https://osf.io/295qp/), phylogenetic reconstructions using constraint trees (https://osf.io/vhup5/), divergence dating in BEAST using a fixed starting tree topology (https://osf.io/7y59t/), Bayesian ancestral state reconstructions using BEAST (https://osf.io/dybu3/), trait-dependent diversification analyses of empirical data using HiSSE (https://osf.io/akcpb/), and trait-dependent diversification analyses of simulated trait data using both BiSSE and HiSSE (https://osf.io/pvq7x/). The alignment files for the sequence capture data and the GenBank data are also available here (https://osf.io/ykthm/). The R scripts required to run the empirical HiSSE analyses are also available on github (https://github.com/dportik/HiSSE_for_Afrobatrachia). The concatenated GenBank alignment and resulting time-calibrated phylogeny are also available on TreeBase (http://purl.org/phylo/treebase/phylows/study/TB2:S23981).

References

Ahl E. 1931. Amphibia, Anura III, Polypedatidae. *Das Tierreich* 55:xvi + 477.

Akopyan M., Kaiser K., Vega A., Savant N.G., Owen C.Y., Dudgeon S.R., Robertson J.M. 2018. Melodic males and flashy females: geographic variation in male and female reproductive behavior in red-eyed treefrogs (*Agalychnis callidryas*). Ethology 124:54-64.

Alfaro M.E., Brock C.D., Banbury B.L., Wainwright P.C. 2009. Does evolutionary innovation in pharyngeal jaws lead to rapid lineage diversification in labrid fishes? BMC Evol. Biol. 9:255.

Aljanabi S., Martinez I. 1997. Universal and rapid salt-extraction of high quality genomic DNA for PCR-based techniques. Nucleic Acids Res. 25:4692–4693.

Amiet J.-L. 2012. Les Rainettes du Cameroun (*Amphibiens Anoures*). Saint-Nazaire, France: La Nef des Livres. 591 pp.

AmphibiaWeb. 2019. Available at: amphibiaweb.org. University of California, Berkeley. Accessed May 2018.

Andersson M. 1994. Sexual selection. Princeton (NJ): Princeton University Press.

Backwell P.R.Y., Passmore N.I. 1990. Aggressive interactions and intermale spacing in choruses of the leaf-folding frog, *Afrixalus delicatus*. S. Afr. J. Zool. 25:133–137.

Baele G., Lemey P., Bedford T., Rambaut A., Suchard M.A., Alekseyenko A.V. 2012. Improving the accuracy of demographic and molecular clock model comparison while accommodating phylogenetic uncertainty. Mol. Biol. Evol. 29:2157–2167.

Baele G., Li W.L.S., Drummond A.J., Suchard M.A., Lemey P. 2013. Accurate model selection of relaxed molecular clocks in Bayesian phylogenetics. Mol. Biol. Evol. 30:239–243.

Barraclough T.G., Harvey P.H., Nee S. 1995. Sexual selection and taxonomic diversity in passerine birds. Proc. R. Soc. Lon. B 259:211–215.

Barratt C.D., Lawson L.P., Bittencourt-Silva G.B., Doggart N., Morgan-Brown T., Nagel P., Loader S.P. 2017. A new, narrowly distributed, and critically endangered species of spiny-throated reed frog (Anura: Hyperoliidae) from a highly threatened coastal forest reserve in Tanzania. Herpetol. J. 27:13–24.

Beaulieu J.M., O'Meara B.C. 2016. Detecting hidden diversification shifts in models of trait-dependent speciation and extinction. Syst. Biol. 65:583–601.

Bell R.C., Parra J.L., Badjedjea G., Barej M.F., Blackburn D.C., Burger M., Channing A., Dehling J.M., Greenbaum E., Gvoždík V., Kielgast J., Kusamba C., Lötters S., McLaughlin P.J., Nagy Z.T., Rödel M.-O., Portik D.M., Stuart B.L., VanDerWal J., Zamudio K.R. 2017a. Idiosyncratic responses to climate-driven forest fragmentation and marine incursions in reed frogs from Central Africa and the Gulf of Guinea Islands. Mol. Ecol. 26:5223–5224.

Bell R.C., Webster G.N., Whiting M.J. 2017b. Breeding biology and the evolution of dynamic sexual dichromatism in frogs. J. Evol. Biol. 30:2104–2115.

Bell R.C., Zamudio K.R. 2012. Sexual dichromatism in frogs: natural selection, sexual selection and unexpected diversity. Proc. R. Soc. Lon. B 279:4687–4693.

Berglund A., Rosenqvist G., Svensson I. 1986a. Reversed sex roles and parental energy investment in zygotes of two pipefish (Syngnathidae) species. Mar. Ecol. Prog. Ser. 29:209–215.

Berglund A., Rosenqvist G., Svensson I. 1986b. Mate choice, fecundity and sexual dimorphism in two pipefish species (Syngnathidae). Behav. Ecol. Sociobiol. 19:301–307.

Bi K., Vanderpool D., Singhal S., Linderoth T., Moritz C., Good J.M. 2012. Transcriptome-based exon capture enables highly cost-effective comparative genomic data collection at moderate evolutionary scales. BMC Genomics 13:403.

Bishop P.J., Jennions M.D., Passmore N.I. 1995. Chorus size and call intensity: female choice in the painted reed frog, *Hyperolius marmoratus*. Behaviour 132:721–731.

Blaimer B.B., Mawdsley J.R., Brady S.G. 2018. Multiple origins of sexual dichromatism and aposematism within large carpenter bees. Evolution 72:1874–1889.

Burnham K.P., Anderson D.R. 2002. Model selection and multimodel inference: a practical information-theoretic approach. New York: Springer.

Burns K. 1998. A phylogenetic perspective on the evolution of sexual dichromatism in tanagers (Thraupidae): the role of female versus male plumage. Evolution 52:1219–1224.

Capella-Gutierrez S., Silla-Martinez J.M., Gabaldon T. 2009. trimAl: a tool for automated alignment trimming in large-scale phylogenetic analyses. Bioinformatics 25:1972–1973.

Channing A. 2001. Amphibians of central and southern Africa. Ithaca (NY): Cornell University Press.

Channing A., Hillers A., Lötters S., Rödel M.-O., Schick S., Conradie W., Rödder D., Mercurio V., Wagner P., Dehling J.M., du Preez L.H., Kielgast J., Burger M. 2013. Taxonomy of the super-cryptic *Hyperolius nasutus* group of long reed frogs of Africa (Anura: Hyperoliidae), with descriptions of six new species. Zootaxa 3620:301–350.

Channing A., Howell K.M. 2006. Amphibians of East Africa. Frankfurt, Germany: Edition Chimaira.

Conradie W., Branch W.R., Measey G.J., Tolley K.A. 2012. A new species of *Hyperolius* Rapp, 1842 (Anura: Hyperoliidae) from the Serra da Chela mountains, south-western Angola. Zootaxa 3269:1–17.
Conradie W., Branch W.R., Tolley K.A. 2013. Fifty shades of grey: giving colour to the poorly known Angolan Ashy reed frog (Hyperoliidae: *Hyperolius cinereus*), with the description of a new species. Zootaxa 3635:201–223.
Conradie W., Verbugt L., Portik D.M., Ohler A., Bwong B.A., Lawson L.P. 2018. A new reed frog (Hyperoliidae: *Hyperolius*) from coastal northeastern Mozambique. Zootaxa 4379:177-198.
Daly J.W. 1995. The chemistry of poisons in amphibian skin. In: Eisner T., Meinwald J., editors. Chemical ecology: the chemistry of biotic interaction. Washington (DC): National Academy Press. p. 17–28.
Darwin C.R. 1871. The descent of man, and selection in relation to sex. Vol. 1. 1st ed. London: John Murray.
De Lisle S.P., Rowe L. 2013. Correlated evolution of allometry and sexual dimorphism across higher taxa. Am. Na.t 183:630–639.
Dehling J.M. 2012. An African glass frog: a new *Hyperolius* species (Anura: Hyperoliidae) from Nyungwe National Park, southern Rwanda. Zootaxa 3391:52–64.
Dominey W. 1984. Effects of sexual selection and life history on speciation: species flocks in African cichlids and Hawaiian *Drosophila*. In: Echelle A.A., Kornfield I., editors. Evolution of fish species flocks. Orono: University of Maine Press. p. 231–249.
Drewes R.C., Vindum J.V. 1994. Amphibians of the impenetrable forest, Southwest Uganda. J. Afr. Zool. 108:55–70.
Drummond A.J., Suchard M.A., Xie D., Rambaut A. 2012. Bayesian phylogenetics with BEAUti and the BEAST 1.7. Mol. Biol. Evol. 29:1969–1973.
Duellman W.E., Trueb L. 1986. Biology of amphibians. New York (NY): McGraw-Hill.
Dunn P.O., Armenta J.K., Whittingham L.A. 2015. Natural and sexual selection act on different axes of variation in avian plumage color. Sci. Adv. 1:e1400155.
Dyson M.L., Passmore N.I. 1988. Two-choice phonotaxis in *Hyperolius marmoratus* (Anura: Hyperoliidae): the effect of temporal variation in presented stimuli. Anim. Behav. 36:648–652.
Dyson M.L., Passmore N.I., Bishop P.J., Henzi S.P. 1992. Male behavior and correlates of mating success in a natural population of African painted reed frogs (*Hyperolius marmoratus*). Herpetologica 48:236–246.
Edgar R.C. 2004. MUSCLE: multiple sequence alignment with high accuracy and high throughput. Nucleic Acids Res. 32:1792–1797.
Eens M., Pinxten R. 2000. Sex-role reversal in vertebrates: behavioural and endocrinological accounts. Behav. Process 51:135–147.
Feng Y.-J., Blackburn D.C., Liang D., Hillis D.M., Wake D.B., Cannatella D.C., Zhang P. 2017. Phylogenomics reveals rapid, simultaneous diversification of three major clades of Gondwanan frogs at the Cretaceous-Paleogene boundary. Proc. Natl. Acad. Sci. USA 114:E5864–E5870.
FitzJohn R.G. 2012. Diversitree: comparative phylogenetic analyses of diversification in R. Methods Ecol. Evol. 3:1084–1092.
FitzJohn R.G., Maddison W.P., Otto S.P. 2009. Estimating trait-dependent speciation and extinction rates from incompletely resolved phylogenies. Syst. Biol. 58:595–611.
Gerhardt H.C. 1994. The evolution of vocalization in frogs and toads. Annu. Rev. Ecol. Syst. 25:233–324.
Gerhardt H.C., Huber F. 2002. Acoustic communication in insects and anurans: common problems and diverse solutions. Chicago (IL): The University of Chicago Press.
Gilbert C.M., Bell R.C. 2018. Evolution of advertisement calls in an island radiation of African reed frogs. Biol. J. Linn. Soc. 123:1–11.
Gomez D., Richardson C., Lengagne T., Derex M., Plenet S., Joly P., Léna J.-P., Théry M. 2010. Support for a role of colour vision in mate choice in the nocturnal European treefrog. Behaviour 147:1753–1768.
Gomez D., Richardson C., Lengagne T., Plenet S., Joly P., Léna J.-P., Théry M. 2009. The role of nocturnal vision in mate choice: females prefer conspicuous males in the European tree frog (*Hyla arborea*). Proc. Biol. Sci. 276:2351–2358.
Grafe T.U. 1997. Costs and benefits of mate choice in the lek-breeding reed frog, *Hyperolius marmoratus*. Anim. Behav. 53:1103–1117.
Greenbaum E., Sinsch U., Lehr E., Valdez F., Kusamba C. 2013. Phylogeography of the reed frog *Hyperolius castaneus* (Anura: Hyperoliidae) from the Albertine Rift of Central Africa: implications for taxonomy, biogeography and conservation. Zootaxa 3131:473–494.
Han X., Fu J. 2013. Does life history shape sexual size dimorphism in anurans? A comparative analysis. BMC Evol. Biol. 13:27.
Harrington S., Reeder T.W. 2017. Rate heterogeneity across Squamata, misleading ancestral state reconstruction and the importance of proper null model specification. J. Evol. Biol. 30:313–325.
Hayes T.B. 1997. Hormonal mechanisms as potential constraints on evolution: examples from the Anura. Am. Zool. 37:482–490.
Hayes T.B., Menendez K.P. 1999. The effect of sex steroids on primary and secondary sex differentiation in the sexually dichromatic reedfrog (*Hyperolius argus*: Hyperolidae) from the Arabuko Sokoke forest of Kenya. Gen. Comp. Endocr. 115:188–199.
Heinsohn R., Legge S., Endler J.A. 2005. Extreme reversed sexual dichromatism in a bird without sex role reversal. Science 309:617–619.
Hofmann C.M., Cronin T.W., Omland K.E. 2008. Evolution of sexual dichromatism. 1. Convergent losses of elaborate female coloration in New World orioles (*Icterus* spp.). Auk 125:778–789.
Huang H., Rabosky D.L. 2014. Sexual selection and diversification: reexamining the correlation between dichromatism and speciation rate in birds. Am. Nat. 184(5):E104–E114.
Jacobs L.E., Vega A., Dudgeon S., Kaiser K., Robertson J.M. 2016. Local not vocal: assortative female choice in divergent populations of red-eyed treefrogs, *Agalychnis callidryas* (Hylidae: Phyllomedusinae). Biol. J. Linn. Soc. 120:171–178.
Jeckel A.M., Grant T., Saporito R.A. 2015. Sequestered and synthesized chemical defenses in the poison frog *Melanophryniscus moreirae*. J. Chem. Ecol. 41:505–512.
Jennions M.D., Bishop P.J., Backwell P.R.Y., Passmore N.I. 1995. Call rate variability and female choice in the African frog, *Hyperolius marmoratus*. Behaviour 132:709–720.
Johnson A.E., Price J.J., Pruett-Jones S. 2013. Different modes of evolution in males and females generate dichromatism in fairy-wrens (Maluridae). Ecol. Evol. 3:3030–3046.
Katoh K., Standley D.M. 2013. MAFFT multiple sequence alignment software version 7: improvements in performance and usability. Mol. Biol. Evol. 30:722–780.
Katoh K., Kuma K., Toh H., Miyata T. 2005. MAFFT version 5: improvement in accuracy of multiple sequence alignment. Nucleic Acids Res. 33:511–518.
Katoh K., Misawa K., Kuma K., Miyata T. 2002. MAFFT: a novel method for rapid multiple sequence alignment based on fast Fourier transform. Nucleic Acids Res. 30:3059–3066.
Kazancıoglu E., Near T.J., Hanel R., Wainwright P.C. 2009. Influence of sexual selection and feeding functional morphology on diversification rate of parrotfishes. Proc. R. Soc. B. 276:3439–3446.
Kimball R.T., Braun E.L., Ligon J.D., Lucchini V., Randi E. 2001. A molecular phylogeny of the peacock-pheasants (Galliformes: *Polyplectron* spp.) indicates loss and reduction of ornamental traits and display behaviours. Biol. J. Linn. Soc. 73:187–198.
Kimball R.T., Ligon J.D. 1999. Evolution of avian plumage dichromatism from a proximate perspective. Am. Nat. 154:182–193.
Kindermann C., Hero J.-M. 2016. Rapid dynamic colour change is an intrasexual signal in a lek breeding frog (*Litoria wilcoxii*). Behav. Ecol. Sociobiol. 70:1995–2003.
King B., Lee M.S.Y. 2015. Ancestral state reconstruction, rate heterogeneity, and the evolution of reptile viviparity. Syst. Biol. 64:532–544.
Kirkpatrick M. 1982. Sexual selection and the evolution of female choice. Evolution 36:1–12.
Kouamé A.M., Kouamé N'.G.G., Konan J.C.B.Y.N'G, Adepo-Gourène B., Rödel M.-O. 2015. Contributions to the reproductive biology and behaviour of the dotted reed frog, *Hyperolius guttulatus*, in southern-central Ivory Coast, West Africa. Herpetol. Notes 8:633–641.
Kouamé N'.G.G., Boateng C.O., Rödel M.-O. 2013. A rapid survey of the amphibians from the Atewa Range Forest Reserve, Eastern Region, Ghana. In: Conservation International, editor. A rapid biological assessment of the Atewa Range Forest Reserve, Eastern Ghana. Conservation International Arlington, Virginia. p. 76–83.

Kraaijeveld K., Kraaijeveld-Smit F.J.L., Maan M.E. 2011. Sexual selection and speciation: the comparative evidence revisited. Biol. Rev. 86:367–377.
Kurabayashi A., Sumida M. 2013. Afrobatrachian mitochondrial genomes: genome reorganization, gene rearrangement mechanisms, and evolutionary trends of duplicated and rearranged genes. BMC Genomics 14:633.
Lande R. 1981. Models of speciation by sexual selection on polygenic traits. Proc. Natl. Acad. Sci. USA 78:3721–3725.
Lande R. 1982. Rapid origin of sexual isolation and character displacement in a cline. Evolution 36:213–223.
Lewis P.O. 2001. A likelihood approach to estimating phylogeny from discrete morphological character data. Syst. Biol. 50:913–925.
Liedtke H.C., Hügil D., Dehling J.M., Pupin F., Menegon M., Plumptre A.J., Kujirakwinja D., Loader S.P. 2014. One or two species? On the case of *Hyperolius discodactylus* Ahl, 1931 and *H. alticola* Ahl, 1931 (Anura: Hyperoliidae). Zootaxa 3768:253–290.
Liu L., Yu L., Edwards S.V. 2010. A maximum pseudo-likelihood approach for estimating species trees under the coalescent model. BMC Evol. Biol. 10:302.
Loader S.P., Ceccarelli F.S., Menegon M., Howell K.M., Kassahun R., Mengistu A.A., Saber S.A., Gebresenbet F., de Sa R., Davenport T.R.B., Larson J.G., Müller H., Wilkinson M., Gower D.J. 2014. Persistence and stability of Eastern Afromontane forests: evidence from brevicipitid frogs. J. Biogeogr. 41:1781–1792.
Loader S.P., Lawson L.P., Portik D.M., Menegon M. 2015. Three new species of spiny throated reed frogs (Anura: Hyperoliidae) from evergreen forests of Tanzania. BMC Res. Notes 8:167.
Luiselli L., Bikikoro L., Odegbune E., Wariboko S.M., Rugiero L., Akani G.C., Politano E. 2004. Feeding relationships between sympatric Afrotropical frogs (genus *Hyperolius*): the effects of predator body size and season. Anim. Biol. 54:293–302.
Maan M.E., Cummings M.E. 2009. Sexual dimorphism and directional sexual selection on aposematic signals in a poison frog. Proc. Natl. Acad. Sci. USA. 106:19072–19077.
Maddison W.P., Midford P.E., Otto S.P. 2007. Estimating a binary character's effect on speciation and extinction. Syst. Biol. 56:701–710.
McDiarmid R.W. 1975. Glass frog romance along a tropical stream. Nat. Hist. Mus. Los Angeles Co Terra 13(4):14–18.
Mendelson T.C., Shaw K.L. 2012. The (mis)concept of species recognition. Trends Ecol. Evol. 27:421–427.
Meyer M., Kircher M. 2010. Illumina sequencing library preparation for highly multiplexed target capture and sequencing. Cold Spring Harb. Protoc. 2010:pdb.prot5448.
Mirarab S., Reaz R., Bayzid M.D.S., Zimmermann T., Swenson M.S., Warnow T. 2014. ASTRAL: genome-scale coalescent-based species tree estimation. Bioinformatics 30:i541–i548.
Mirarab S., Warnow T. 2015. ASTRAL-II: coalescent-based species tree estimation with many hundreds of taxa and thousands of genes. Bioinformatics 31:i44–i52.
Misof B. 2002. Diversity of Anisoptera (Odonata): inferring speciation processes from patterns of morphological diversity. Zoology 105:355–365.
Morrow E.H., Pitcher T.E., Anrqvist G. 2003. No evidence that sexual selection is an 'engine of speciation' in birds. Ecol. Lett. 6:228–234.
Nali R.C., Zamudio K.R., Haddad C.F.B., Prado C.P.A. 2014. Size-dependent selective mechanisms on males and females and the evolution of sexual size dimorphism in frogs. Am. Nat. 184:727–740.
Omland K.E. 1997. Examining two standard assumptions of ancestral reconstructions: repeated loss of dichromatism in dabbling ducks. Evolution 51:1636–1646.
Oring L.W. 1982. Avian mating systems. In: Farner DS, King JS, Parkes KC, editors. Avian Biology. New York (NY): Academic Press. p. 1–92.
Owens I.P.F., Bennett P.M., Harvey P.H. 1999. Species richness among birds: body size, life history, sexual selection or ecology? Proc. R. Soc. Lon. B 266:933−939.
Palumbi S., Martin A., Romano S., McMillan W.O., Stice L., Grabowski G. 1991. The simple fool's guide to PCR. Version 2. Honolulu: University of Hawaii.
Panhuis T.M., Butlin R., Zuk M., Tregenza T. 2001. Sexual selection and speciation. Trends Ecol. Evol. 16:364–371.
Paradis E., Claude J., Strimmer K. 2004. APE: analysis of phylogenetics and evolution in R language. Bioinformatics 20:289–290.
Phillimore A.B., Freckleton R.P., Orme C.D.L., Owens I.P.F. 2006. Ecology predicts large-scale patterns of phylogenetic diversification in birds. Am. Nat. 168:220–229.
Portik D.M. 2015. Diversification of afrobatrachian frogs and the herpetofauna of the Arabian Peninsula [PhD Thesis]. Berkeley (CA): University of California.
Portik D.M., Blackburn D.C. 2016. The evolution of reproductive diversity in Afrobatrachia: a phylogenetic comparative analysis of an extensive radiation of African frogs. Evolution 70: 2017–2032.
Portik D.M., Jongsma G.F., Kouete M.T., Scheinberg L.A., Freiermuth B., Tapondjou W.P., Blackburn D.C. 2016a. A survey of amphibians and reptiles in the foothills of Mount Kupe, Cameroon. Amphib. Reptile Conserv. 10(2)[Special Section]:37–67(e131).
Portik D.M., Jongsma G.F., Kouete M.T., Scheinberg L.A., Freiermuth B., Tapondjou W.P., Blackburn D.C. 2018. Ecological, morphological, and reproductive aspects of a diverse assemblage of hyperoliid frogs (Family: Hyperoliidae) surrounding Mt. Kupe, Cameroon. Herpetol. Rev. 49:397–408.
Portik D.M., Scheinberg L., Blackburn D.C., Saporito R.A. 2015. Lack of defensive alkaloids in the integumentary tissue of four brilliantly colored African reed frog species (Hyperoliidae: *Hyperolius*). Herpetol. Conserv. Biol. 10:833–838.
Portik D.M., Smith L.L., Bi K. 2016b. An evaluation of transcriptome-based exon capture for frog phylogenomics across multiple scales of divergence (Class: Amphibia, Order: Anura). Mol. Ecol. Resour. 16:1069–1083.
Portik D.M., Smith L.L., Bi K. 2016c. Data from: An evaluation of transcriptome-based exon capture for frog phylogenomics across multiple scales of divergence (Class: Amphibia, Order: Anura). Dryad Digital Repository. https://doi.org/10.5061/dryad.pr3pr
Price J.J., Eaton M.D. 2014. Reconstructing the evolution of sexual dichromatism: current color diversity does not reflect past rates of male and female change. Evolution 68:2026–2037.
Price T. 2008. Sexual selection and natural selection in bird speciation. Phil. Trans. R. Soc. Lond. B 353:251–260.
Price T., Birch G.L. 1996. Repeated evolution of sexual color dimorphism in passerine birds. Auk 113:842–848.
Pyron R.A., Wiens J.J. 2011. A large-scale phylogeny of Amphibia including over 2800 species, and a revised classification of extant frogs, salamanders, and caecilians. Mol. Phylogenet. Evol. 61:543–583.
Rabosky D.L., Goldberg E.E. 2015. Model inadequacy and mistaken inferences of trait-dependent speciation. Syst. Biol. 64:340–355.
Rambaut A., Drummond A.J., Suchard M. 2013. Tracer v1.6.0. Available from: http://beast.bio.ed.ac.uk/
Revell L.J. 2012. Phytools: an R package for phylogenetic comparative biology (and other things). Methods Ecol. Evol. 3:217–223.
Richards C.M. 1982. The alteration of chromatophore expression by sex hormones in the Kenyan Reed Frog, *Hyperolius viridiflavus*. Gen. Comp. Endocr. 46:59–67.
Ritchie M.G. 2007. Sexual selection and speciation. Ann. Rev. Ecol. Evol. Syst. 38:79–102.
Rödel M.-O., Grafe T.U., Rudolf V.H.W., Ernst R. 2002. A review of West African spotted *Kassina*, including a description of *Kassina schioetzi* sp. nov. (Amphibia: Anura: Hyperoliidae). Copeia 2002:800–814.
Rödel M.-O., Kosuch J., Grafe T.U., Boistel R., Assemian N.E., Kouamé N.G., Tohé B., Gourène G., Perret J.-L., Henle K., Tafforeau P., Pollet N., Veith M. 2009. A new tree-frog genus and species from Ivory Coast, West Africa (Amphibia: Anura: Hyperoliidae). Zootaxa 2044:23–45.
Rödel M.-O., Kosuch J., Veith M., Ernst R. 2003. First record of the genus *Acanthixalus* Laurent, 1944 from the Upper Guinean Rain Forest, West Africa, with the description of a new species. J. Herpetol. 37:43–52.
Rödel M.-O., Sandberger L., Penner J., Mané Y., Hillers A. 2010. The taxonomic status of *Hyperolius spatzi* Ahl, 1931 and *Hyperolius nitidulus* Peters, 1875 (Amphibia: Anura: Hyperoliidae). Bonn. Zool. Bull. 57:177–188.
Roede M. 1972. Color as related to size, sex and behavior in seven Caribbean labrid fish species (genera *Thalasoma, Halichoeres* and *Hemipteronotus*). Studies on the Fauna of Curacao and other Caribbean Islands 42:1–266.

Roelants K., Gower D.J., Wilkinson M., Loader S.P., Biju S.D., Guillaume K., Moriau L., Bossuyt F. 2007. Global patterns of diversification in the history of modern amphibians. Proc. Natl. Acad. Sci. USA 104:887–892.

Rojas B. 2017. Behavioural, ecological, and evolutionary aspects of diversity in frog colour patterns. Biol. Rev. 92:1059–1080.

Ryan M.J. 1980. Female choice in a Neotropical frog. Science 209:523–525.

Safran R.J., Scordato E.S.C., Symes L.B., Rodríguez R.L., Mendelson T.C. 2013. Contributions of natural and sexual selection to the evolution of premating reproductive isolation: a research agenda. Trends Ecol. Evol. 28:643–650.

Salthe S.N., Duellman W.E. 1973. Quantitative constraints associated with reproductive mode in anurans. In: Vial J.L., editor. Evolutionary Biology of the Anurans. Missouri: University of Missouri Press. p. 229–249.

Sanderson M.J. 2002. Estimating absolute rates of molecular evolution and divergence times: a penalized likelihood approach. Mol. Biol. Evol. 19:101–109.

Saporito R.A., Donnelly M.A., Madden A.A., Garraffo H.M., Spande T.F. 2010. Sex-related differences in alkaloid defenses of the dendrobatid frog *Oophaga pumilio* from Cayo Nancy, Bocas del Toro, Panama. J. Nat. Prod. 73:317–321.

Saporito R.A., Donnelly M.A., Spande T.F., Garraffo H.M. 2012. A review of chemical ecology in poison frogs. Chemoecology 22:159–168.

Sayyari E. Mirarab S. 2016. Fast coalescent-based computation of local branch support from quartet frequencies. Mol. Biol. Evol. 33:1654–1668.

Schick S., Kielgast J., Rödder D., Muchai V., Burger M., Lötters S. 2010. New species of reed frog from the Congo Basin with discussion of paraphyly in cinnamon-belly reed frogs. Zootaxa 2501:23–36.

Schiøtz A. 1967. The treefrogs (Rhacophoridae) of West Africa. Spolia Zoologica Musei Hauniensis 25:1–346.

Schiøtz A. 1999. Treefrogs of Africa. Frankfurt, Germany: Edition Chimaira.

Seddon N., Botero C.A., Tobias J.A., Dunn P.O., MacGregor H.E.A., Rubenstein D.R., Uy A.C., Weir J.T., Whittingham L.A., Safran R.J. 2013. Sexual selection accelerates signal evolution during speciation in birds. Proc. Biol. Sci. 280:20131065.

Selander R.K. 1966. Sexual dimorphism and differential niche utilization in birds. Condor 68:113–151.

Seo T.-K. 2008. Calculating bootstrap probabilities of phylogeny using multilocus sequence data. Mol. Biol. Evol. 25:960–971.

Shine R. 1979. Sexual selection and sexual dimorphism in the Amphibia. Copeia 1979:297–306.

Shine R. 1989. Ecological causes for the evolution of sexual dimorphism: a review of the evidence. Q. Rev. Biol. 64:419–461.

Shultz A.J., Burns K.J. 2017. The role of sexual and natural selection in shaping patterns of sexual dichromatism in the largest family of songbirds (Aves: Thraupidae). Evolution 71:1061–1074.

Singhal S. 2013. De novo transcriptomic analyses for non-model organisms: an evaluation of methods across a multi-species data set. Mol. Ecol. Resour. 13:403–416.

Stamatakis A. 2014. RAxML version 8: a tool for phylogenetic analysis and post-analysis of large phylogenies. Bioinformatics 30:1312–1313.

Starnberger I., Poth D., Peram P.S., Schulz S., Vences M., Knudsen J., Barej M.F., Rödel M.-O., Walzl M., Hödl W. 2013. Take time to smell the frogs: vocal sac glands of reed frogs (Anura: Hyperoliidae) contain species-specific chemical cocktails. Biol. J. Linn. Soc. 110:828–838.

Starnberger I., Preininger D., Hödl W. 2014. From uni- to multimodality: towards an integrative view on anuran communication. *J. Comp. Physiol. A* 200:777–787.

Stuart-Fox D., Owens I.P.F. 2003. Species richness in agamid lizards: chance, body size, sexual selection or ecology? J. Evol. Biol. 16:659–669.

Sztatecsny M., Preininger D., Freudmann A., Loretto M.-C., Maier F., Hödl W. 2012. Don't get the blues: conspicuous nuptial colouration of male moor frogs (*Rana arvalis*) supports visual mate recognition during scramble competition in large breeding aggregations. Behav. Ecol. Sociobiol. 66:1587–1593.

Telford S.R. 1985. Mechanisms of evolution and inter-male spacing in the painted reedfrog *(Hyperolius marmoratus)*. Anim. Behav. 33:1353–1361.

Telford S.R., Dyson M.L. 1988. Some determinants of the mating system in a population of painted reed frogs (*Hyperolius marmoratus*). Behaviour 106:265–278.

Telford S.R., Passmore N.I. 1981. Selective phonotaxis of four sympatric species of African reed frogs (genus *Hyperolius*). Herpetologica 37:29–32.

Toledo L.F., Haddad C.F.B. 2009. Colors and some morphological traits as defensive mechanisms in anurans. Int. J. Zool. 2009:910892.

Turelli M., Barton N.H., Coyne J.A. 2001. Theory and speciation. Trends Ecol. Evol. 16:330–342.

Veith M., Kosuch J., Rödel M.-O., Hillers A., Schmitz A., Burger M., Lötters S. 2009. Multiple evolution of sexual dichromatism in African reed frogs. Mol. Phylogenet. Evol. 51:388–393.

Wagner C.E., Harmon L.J., Seehausen O. 2012. Ecological opportunity and sexual selection together predict adaptive radiation. Nature 487:366–369.

Wells K.D. 1977. The social behavior of anuran amphibians. Anim. Behav. 25:666–693.

West-Eberhard M.J. 1983. Sexual selection, social competition, and speciation. Q. Rev. Biol. 58:155–183.

Wieczorek A., Drewes R., Channing A. 2000. Biogeography and evolutionary history of *Hyperolius* species: application of molecular phylogeny. J. Biogeogr. 27:1231–1243.

Wollenberg K.C., Glaw F., Meyer A., Vences M. 2007. Molecular phylogeny of Malagasy reed frogs, *Heterixalus*, and the relative performance of bioacoustics and color-patterns for resolving their systematics. Mol. Phylogenet. Evol. 45:14–22.

Woolbright L.L. 1983. Sexual selection and size dimorphism in anuran Amphibia. Am. Nat. 121:110–119.

Yovanovich C.A.M., Koskela S.M., Nevala N., Kondrashev S.L., Kelber A., Donner K. 2017. The dual rod system of amphibians supports colour discrimination at the absolute visual threshold. Phil. Trans. R. Soc. 372:20160066.

Zhang C., Sayyari E., Mirarab S. 2017. ASTRAL-III: increased scalability and impacts of contracting low support branches. In: Meidanis J, Nakhleh L, editors. Comparative Genomics. RECOMB-CG 2017. Lecture Notes in Computer Science, vol. 10562. Cham: Springer. p. 53–75.